Title:

Local and non-local effects of building arrangements on pollutant fluxes within the urban canopy

Authors:

E V Goulart[1], N C Reis Jr[1], V F Lavor[1], Ian P Castro[2], J M Santos[1,*], Z. T. Xie[2]

Affiliations:

1. Department of Environmental Engineering, Universidade Federal do Espírito Santo, Brazil, Av. Fernando Ferrari 514, 29.075-910 Vitoria – ES, Brazil
2. Faculty of Engineering and the Environment, University of Southampton, Highfield, Southampton SO17 1BJ, UK

Abstract: This work investigates the vertical and horizontal mass (scalar) flux of a contaminant emitted from an area source located in an array of blocks representing an urban environment. Arrays consisting of buildings with random and uniform heights and staggered and aligned arrangements were tested. Results shows that the vertical scalar flux close to the source can affect downwind clean zones. It is also shown that taller buildings increase the vertical scalar flux and the fluctuations of the vertical velocity above the smaller buildings. The vertical advective scalar flux was found to have an effect on dispersion in the vicinity of the building (a local effect), while the vertical turbulent fluxes are associated with pollutant transportation downwind above the smaller buildings (a non-local effect).

Keywords: urban areas, dispersion, vertical scalar fluxes, random building height

1. Introduction

The wind flow over urban environments is affected by the geometrical features of buildings which in turn influence the vertical and horizontal fluxes of pollutants within the urban canopy and above. This influence can be seen locally in the vicinity of each building and also in the pollutants' transport from one region of the urban area to another further away.

Numerous experimental studies and numerical investigations have focused on understanding the wind flow and air pollutants dispersion affected by the presence of a buildings array which represents urban environments (Cheng and Castro, 2002; Coceal et al., 2006 and 2007; Xie et al., 2008; Pascheke et al., 2008; Boppana et al., 2010; Branford et al., 2011; Castro et al., 2017; Fuka et al., 2017; Kikumoto and Ooka, 2018; Carpentieri et al., 2018; among others). These can help urban planning for air quality improvement by supporting the choice of a more appropriate urban configuration in terms of the positioning of buildings and their three-dimensional characteristics (Yuan et al., 2014), or give support for building emergency plans in case of accidental or intentional releases of contaminants (Soulhac et al., 2011 and Soulhac et al., 2012).

The presence of buildings, especially tall buildings, disturbs the atmospheric flow considerably. Tominaga and Stathopoulos (2016) presented a review of near-field pollutant dispersion in built environments in which they explained the interaction between buildings and dispersion. Direct Numerical Simulation (DNS) of flow (Coceal et al., 2006 and 2007) and dispersion (Branford et al., 2011) of a passive pollutant emitted by a point source located within an array of cubic-like buildings revealed that the most significant processes controlling dispersion in urban areas are channelling flow along the streets, topological dispersion due to the presence of buildings (Branford et al 2011, Coceal et al 2014, Yevgeny et al 2007), plume skewing due to the flow turning with height, detrainment by turbulent dispersion, entrainment to building wakes, and development of secondary sources.

Recently, Goulart et al. (2017), using the same set of DNS data as Branford et al. (2011), investigated pollutant dispersion within and above the urban canopy. The results showed that the vertical pollutant mass (scalar) flux within the urban canopy is dominated by the turbulent component. On the other hand, the horizontal scalar flux below the canopy is dominated by advection while above the canopy there is a counter-gradient part of the turbulent horizontal scalar flux. As pointed out by Goulart et al. (2017), the vertical flux has an important role on how pollutants spreads through the array. Initial detrainment reduces pollutant concentration within the array. However, re-entrainment could increase concentration further away from the source.

Large Eddy Simulation (LES) has been used in numerical investigations of turbulent flow over an array of buildings. Xie et al. (2008), Fuka et al. (2017) and Castro et al. (2017) have shown that LES can yield excellent agreement with experimental and DNS data and therefore can be a reliable tool to investigate building-affected dispersion. Another recent example of LES reliability in modeling atmospheric turbulence in urban areas is the work of Yoshida et al. (2018) who used it to investigate the effects of building height variability on turbulent flows in the lower part of the urban boundary layer in Kyoto, comparing results to field experimental data. They showed that the plan-area index λ_p (the ratio of the plan area occupied by buildings to the total surface area) is an important parameter in distinguishing the effects of building height variability. A threshold for the influence of height randomness on turbulence variables become evident on flow and dispersion. It means that for sparsely populated (of buildings) sites, with $\lambda_p < 0.17$ according to Zaki *et al.* (2011), the height variability effects are not important. Our three simulated cases have $\lambda_p = 0.25$, so it is important to study the heights randomness effects.

A series of studies investigate how the high-rise building affects the flow and dispersion in pedestrian level. Aristodemou et al (20018) used wind tunnel and numerical simulation to investigate the effect of a tall building in flow and dispersion in a neighbourhood area. They found that the tall buildings affected the surrounding air flows and dispersion patterns, with the generation of "dead-zones" and high concentration "hotspots" in areas where these did not previously exist.

Hang and Li (2010) and Hang et al. (2011) investigated the flow and ventilation rates over array with high-rise building. They found that the ventilation rates decrease over arrays with tall buildings. While building height variation enhance vertical mean flows

and therefore enhance the vertical ventilation in comparison to uniform buildings heights.
Hang et al (2012) studied pollutant dispersion over arrays with high-rise building. They found that, regarding pollutant removal, for canopies with the same average height (with different building height), the effects of turbulent diffusions are less important than the horizontal and vertical mean flow. They also pointed that as the standard deviation of the building heights increases, it lowers the pedestrian level concentration.

Fuka et al. (2017) used LES to investigate the fluid flow and dispersion of pollutants emitted from a ground point source within an array of buildings containing a tall one. They showed that the taller building significantly alters the flow field and can enhance or reduce the vertical scalar transfer depending on the location of the ground source relative to the tall building. These results agree with similar findings obtained by numerical simulations of wind flow over different urban configurations reported by Cheng and Castro (2002) and Xie et al. (2008). This also agrees with the results obtained by Boppana et al. (2010) whose work presented results for dispersion from an area source located within urban configurations identical to those used by Cheng and Castro (2002), Xie et al. (2008) and Pascheke et al. (2008) and showed that the dispersion pattern for the random height configuration is more complex than for a uniform height array. These studies have clearly demonstrated that canopy ventilation is very much affected by the surface morphology.

Carpentieri et al. (2018) measured turbulent and advective scalar flux over two arrays of rectangular buildings in a wind tunnel. The first array consisted of uniform height buildings and the second contained buildings of different heights. They also found that advective horizontal scalar fluxes were dominant over the turbulent scalar flux. However, they concluded that the advective and turbulent vertical scalar fluxes have the same order of magnitude. Moreover, the presence of a taller and isolated building upwind of the measurement enhances the vertical scalar transfer but building height variability seems to have an insignificant effect on the vertical scalar transfer, although their plan-area index was $\lambda_p = 0.54$, much greater than the threshold 0.3 suggested by Yoshida et al. (2018).

Therefore, the main aim of this work consists of analyzing how urban configuration affects the advective and turbulent vertical and horizontal fluxes of pollutant. The analysis was conducted considering the effect of taller buildings on the fluxes in their vicinity (a local effect) and downwind above the smaller buildings (a non-local effect). The vertical fluxes in and out of the canopy as well as the horizontal fluxes can help to describe the influence of building height variability and arrangements on the pollutant dispersion. In addition, the partition between advective and turbulent fluxes can be used to determine the characteristic velocity responsible for transporting the pollutants from within the canopy to the boundary layer above. We performed numerical simulations using LES to investigate flow and dispersion in three different urban-like configurations (uniform and random buildings heights in staggered and aligned configurations) in which the source is distributed spatially on the floor.

2. Mathematical Modeling

Figure 1 presents the three configurations considered. The first is a staggered array with random building heights (RBSA) (Figure 1a). The second is an aligned array with random building heights (RBAA) (Figure 1b). Finally, the last configuration is a staggered array with uniform building height (UBSA) (Figure 1c). In both cases of random buildings, the building height distribution follows a Gaussian distribution ranging from 2.8mm to 17.2mm. The computational domain plan area is $24H_m$ x $16H_m$ along the streamwise and spanwise directions, respectively (H_m is the average building height equal to 10mm). To further explore the downwind effects of different building heights and arrangement, the domain length of $24H_m$ is greater than the previous studies of Boppana et al. (2010). Each repeating unit comprised an array of sixteen blocks ($8H_m$ by $8H_m$). Therefore, the domain is one repeating unit longer in the streamwise direction than that of Boppana et al. (2010). The height of the domain is $6H_m$ and $10H_m$ for the uniform and random heights configurations, respectively.

To validate the flow field, the numerical results were compared with the wind tunnel data obtained by Cheng and Castro (2002) and the LES simulations performed by Xie et al. (2008). To validate the concentration field, the numerical results were compared with the wind tunnel data obtained by Pascheke et al. (2008) and the LES simulation performed by Boppana et al. (2010).

Table 1. Characteristic parameters

Configuration	$Re_H = u_H H_m / \nu$	u_H (ms^{-1})	Friction velocity, u_* (ms^{-1})
RBSA	1860.53	1.322	0.571
UBSA	1897.58	1.349	0.442
RBAA	2709.69	1.926	0.571

The freestream flow direction was parallel to the buildings walls (zero degrees) and the Reynolds number is defined as $Re_H = u_H H_m / \upsilon$ where u_H is the domain-averaged velocity at the average building height. Values of Reynolds number and friction velocity are presented in Table 1. Xie and Castro (2006) performed a series of LES simulation over array of buildings with Re varying from 5x103 to 5 x106. They concludes that dependency of the Reynolds number is poor. The weak dependency can be explained because the turbulence production has a comparable scale as the roughness elements. Also, the surface drag is basically due to the pressure related to the shape of the obstacle.

The Reynolds number effect can be important for a wind tunnel size model if skin friction, or surface scalar flux, or surface heat transfer is of interest. This paper is not focused on these. It is to be noted that in this paper, except for the validation, all of the results are presented in dimensionless data normalized by the flux at the source, with a focus on the study on dispersion away from the area source but not in the immediate vicinity of the source. This is governed by the building size scale turbulence, and should not significantly dependent on the Reynolds number.

In the laboratory experiments, naphthalene was coated onto the ground surface of the first repeating units of $8H_m$ x $8H_m$ to represent the area source, see the light blue area in Figure 1. The molecular Schmidt number Sc of naphtalene was assumed to be 2.284, as used by Boppana et al (2010) and Pascheke et al. (2008). An area source in an urban environment could be identified as a small localized zone where accidental or deliberate releases of pollutants or toxic gases can occur or perhaps a zone of heavy vehicle traffic.

Large-eddy simulation was used to simulate incompressible flow with ρ=1.225 kg m^{-3} and $\mu = 8.71\times10^{-6}$ kg m^{-1}s^{-1}. The Smagorinsky-Lilly model, which has a near-wall dumping function, with C_S = 0.1 was used to handle Subgrid scales, with the SGS turbulent Schmidt number taken as Sc_t =0.9 (Xie et al., 2004; Cai et al., 2008). Periodic boundary conditions were imposed in the main wind flow direction and on the lateral boundaries. Flow was maintained with a constant pressure gradient imposed in each control volume, given by $\partial P/\partial x = \rho u_*^2/L$ where u_* is the total wall friction velocity and L is the height of the domain. At all solid surfaces a no-slip boundary condition was applied. At the top of the domain, a free slip condition was applied. The area source was specified by a constant concentration equal to the saturation concentration of naphthalene in air (2x10^{-4} kg m^{-3}). A sponge layer (indicated as a blue line on Figure 1) was applied at the inlet to prevent pollutant mass from entering the domain.

The numerical simulations were performed using the commercial software Fluent Ansys version 18, which employs the finite volume method to discretize the conservation equations. A second order implicit scheme was chosen to discretize the temporal variables and a central differencing scheme was used for spatial discretization. Xie and Castro (2006) indicated that a mesh containing 16 cells over each cube dimension was adequate to simulate the flow past a staggered cube array, while Boppana et al. (2010) suggested that the accurate computation of the scalar fluxes close to the surface requires a much finer grid resolution. Based on grid checks, these authors indicated that a vertical cell size of H_m/64 close to the surface was required. Therefore, to optimize the cell size distribution, an eight million grid point hexahedral mesh was constructed with two mesh refinement regions. In the first region, 0 < z/H_m < 6, in order to accurately model the scalar fluxes close to the surface at the source location, a vertical cell size of H_m/75 resolution close to the surface was used, gradually expanding to H_m/16 (using a power-law), with a constant grid size of H_m/16 in the *x* and *y* directions. In the second region there was a step jump in mesh size , above z/H_m equal to 6, a uniform H_m/8 was used for all directions; since the main interest of this work is the prediction of the transport mechanism inside the building canopy this discontinuity in mesh size was not thought to be significant.

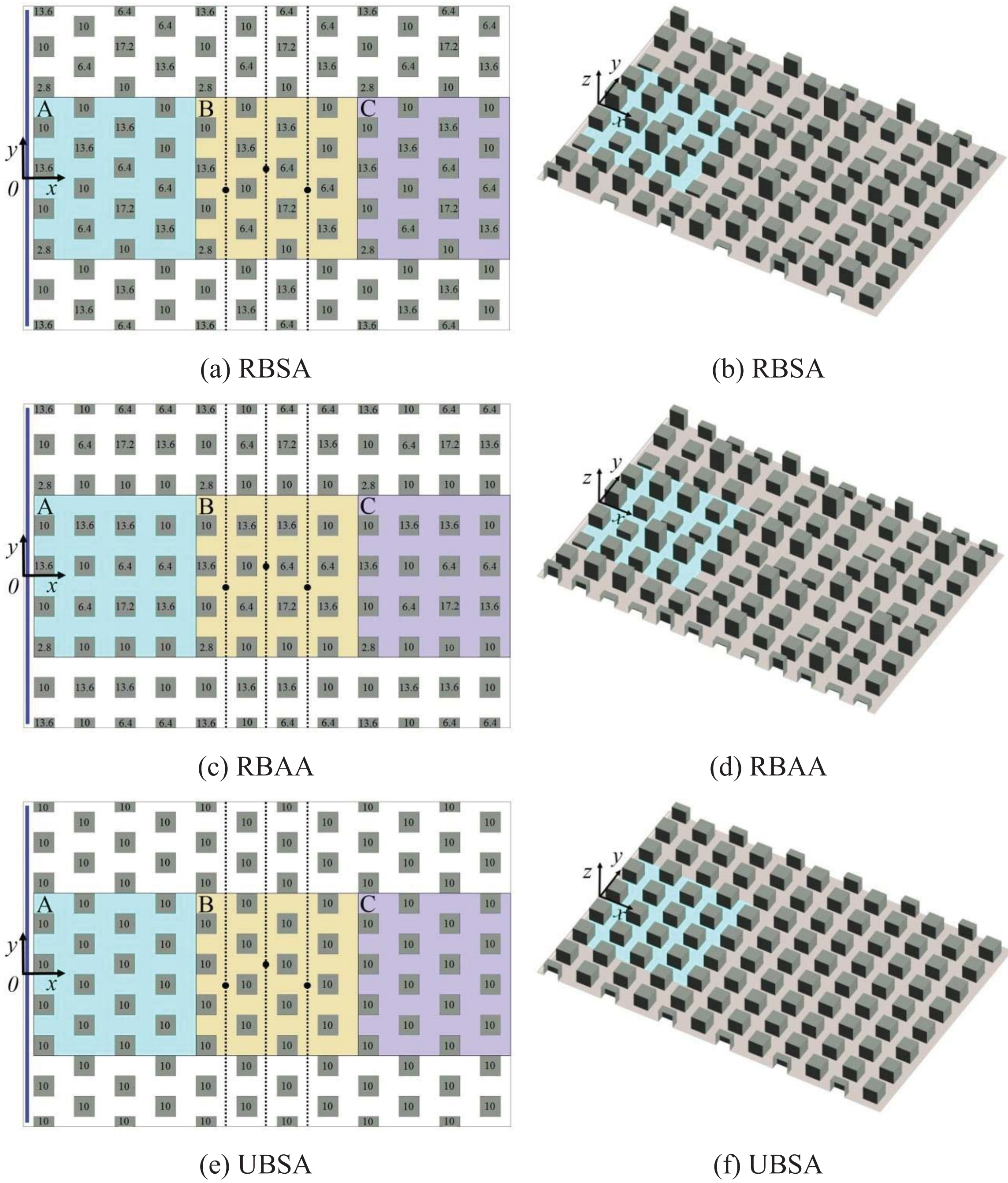

Figure 1. (a), (c) & (e) are plan views of the urban configurations shown in (b), (d) & (f), respectively. The grey squares denote the building positions and the number inside each square denotes the building height in mm. The width in both streamwise and lateral directions of the buildings is 10 mm. The width of the streets is 10 mm. (a) staggered array with random buildings height (RBSA), (b) aligned array with random building height (RBAA) and (c) staggered array with uniform buildings height (UBSA). The regions marked with the capital letters A, B and C (in (a), (c), (e)) denote repeating units comprising sixteen blocks ($8H_m$ by $8H_m$), where the light blue zone (zone A)

coincide with the area source. Black dots show the locations of the vertical concentration profiles.

All simulations had a spin up period for flow and scalar field of at least $80T_C$ (characteristic time was defined as $T_C = H_m/u_*$). The time step for the simulations was $T_S = 0.002T_C$ and the total averaging time was at least $200T_C$ for all simulations.

3. Results and Discussion

The results are divided into three main parts. Firstly, Section 3.1 presents a comparison of the results obtained with previous wind tunnel experiments and LES simulations. Section 3.2 describes the local effects of building heights and arrangement upon the vertical flux of scalar. Finally, Section 3.3 explores the effect of emission over a downstream clean urban zone, discussing the local and non-local effects of the different configurations upon the vertical and streamwise component of the horizontal flux of scalar.

3.1. Comparison with a wind tunnel experiment and LES simulation

Spatially averaged streamwise velocities are presented in Figure 2. This Figure shows a comparison between the results obtained in the present work, the LES results obtained by Xie et al. (2008) and wind tunnel data obtained by Cheng and Castro (2002) for the staggered random height array configuration (RBSA) and the staggered uniform height array configuration (UBSA).

For the RBSA configuration, both LES simulations showed similar velocity profiles. Nevertheless, the velocity was underestimated at the top of the domain if compared with the wind tunnel data. The same result was found by Xie et al. (2008). Although, there are no wind tunnel data for the comparison of these variables in the UBSA configuration, we have chosen to present these results as they helpfully supplement the later comparison of concentration profiles for which wind tunnel data are available. The streamwise velocity profile indicates a stronger velocity gradient in the case of UBSA if compared with the RBSA configuration (Figure 2), which is perhaps not surprising.

Lateral and vertical profiles of concentration are presented for RBSA and UBSA configurations in Figures 3 and 4, respectively. Concentration is shown in non-dimensional form to enable comparison with results from previous works ($C^* = c/c_o$ where c_o is the concentration at the source). It can be seen that the LES results obtained in the present work show good agreement with LES results obtained by Boppana et al. (2010), as well as with experimental data obtained by Pascheke et al. (2008).

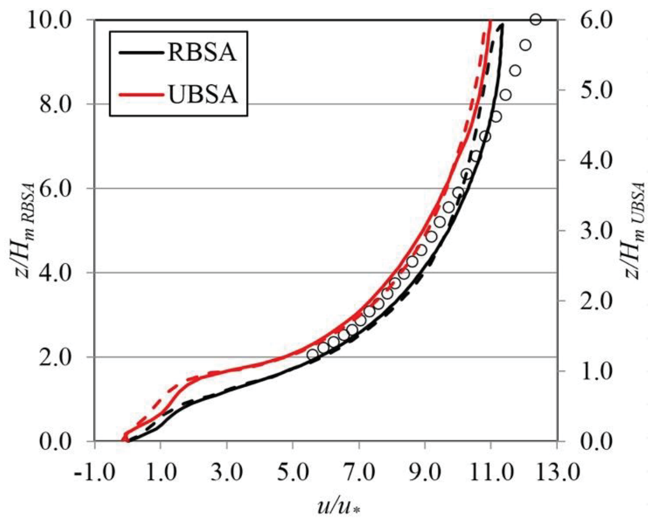

Figure 2. Spatially averaged mean velocity. Circles represent the wind tunnel velocity data obtained by Cheng and Castro (2002). Broken and solid lines indicate the LES velocity results produced by Xie et al. (2008) and in the present work, respectively.

For all configurations, concentrations are expected to decrease with distance from the source. However, for the RBSA configuration, there is a more three-dimensional flow with larger vertical scalar transfer and concentration is therefore expected to decrease more rapidly with distance as seen in Figure 3a. Further from the area source the lateral concentration profiles approach a Gaussian profile. Near the source, the effect of the buildings is more evident, modifying the lateral concentration profiles. For the RBSA configuration the profile showed in Figure 3a resembles a double-peak Gaussian profile due to the presence of a taller building (13.5 *mm*). Examining the uniform height array (UBSA), the concentration profile also approaches a Gaussian profile with distance from the source but does not present the double-peak feature (Figure 3). In this case (UBSA), the concentration peak is higher which indicates less vertical transfer.

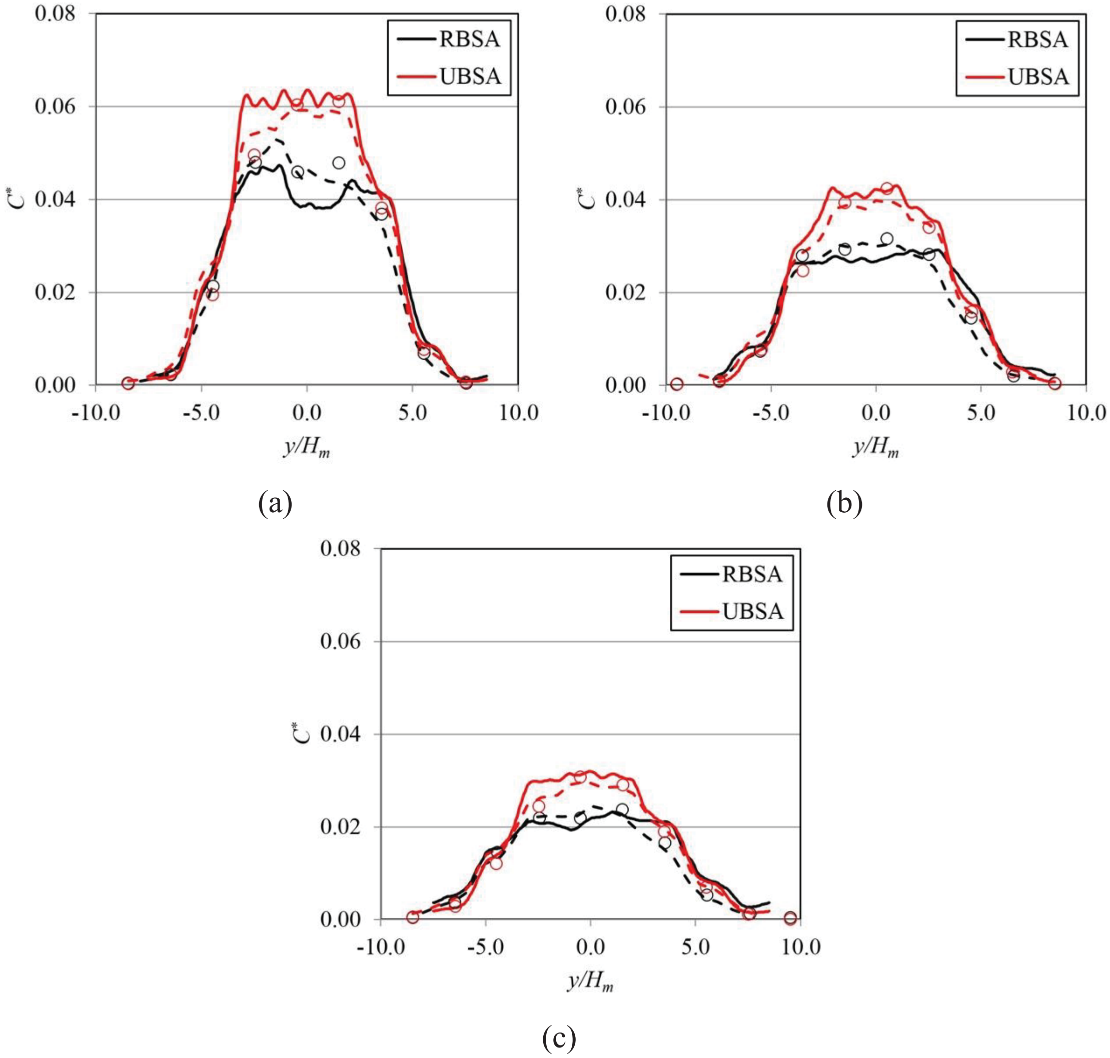

Figure 3. Lateral concentration profile for the RBSA and UBSA configurations calculated at $z/H_m = 0.6$ and three different downstream distances measured from the end of the area source: (a) $x/H_m = 10$, (b) $x/H_m = 12$ and (c) $x/H_m = 14$. Circles represent the wind tunnel concentration data obtained by Pascheke et al. (2008). Broken and solid lines indicate the LES concentration results produced by Boppana et al. (2010) and in the present work, respectively.

The vertical concentration gradient is steeper closer to the area source for all configurations. However, for the UBSA this gradient is even steeper than for the RBSA configuration. Branford et al. (2011) showed DNS results of the flow and dispersion of a ground point source over an array of uniform cubes and found little vertical exchange for cases in which wind direction is parallel to the array. Here, we found that the random building heights enhance the vertical scalar exchange. This is also supported by Castro et al. (2017) and Fuka et al. (2018). We will return to this point later.

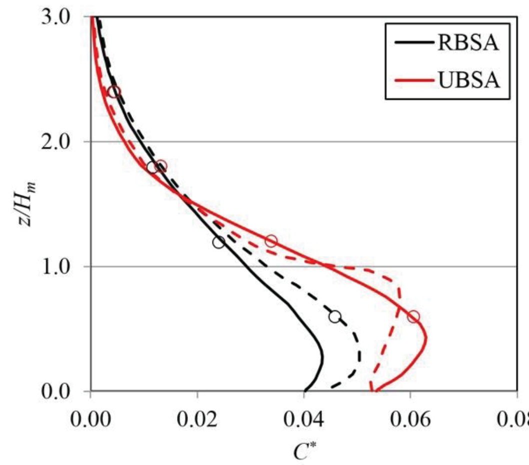

(a)

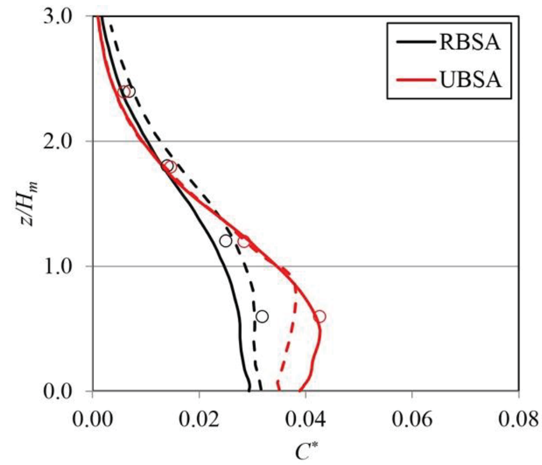

(b)

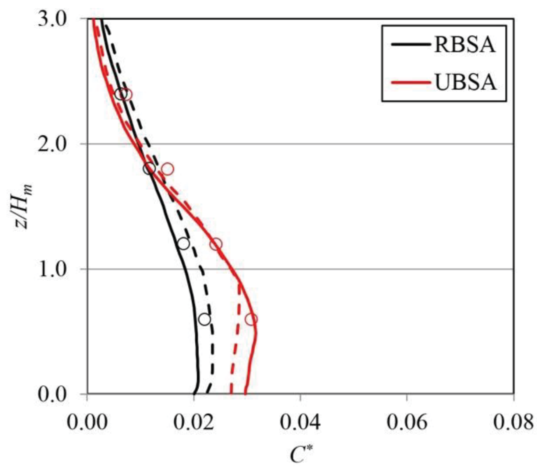

(c)

Figure 4. Vertical concentration profiles measured downstream the source area at (a) $x/H_m = 10$ and y/H_m= -0.5, (b) $x/H_m = 12$, y/H_m= 0.5 and (c) $x/H_m = 14$, y/H_m= -0.5 for the RBSA and UBSA configurations (black dots in Figure 1). Circles represent the wind tunnel concentration data obtained by Pascheke et al. (2008). Broken and solid lines indicate the LES concentration results produced by Boppana et al. (2010) and in the present work, respectively.

3.2 Local effect of pollutants fluxes on dispersion over an array of buildings

To explore the local effects of the differences in building heights on the scalar fluxes, spatially averaged vertical scalar fluxes were calculated as the average of the flux within a squared area at building height, comprising of Lx x Ly = 1H_m x 1H_m for all simulations as indicated in Equation 1, where the total scalar flux is the sum of the advective and turbulent vertical scalar fluxes. Partition of the turbulent and advective scalar fluxes normalized by the time-averaged scalar flux emitted by the source are presented in Figures 5, 7 and 8 for different lines along the array at z/H_m =1.0, for UBSA, RBSA and RBAA, respectively. The averaged scalar fluxes at the source were 6.27 x10^{-6} kg m^{-2} s^{-1}, 7.37x10^{-6} kg m^{-2} s^{-1} and 7.12 x10^{-6} kg m^{-2} s^{-1}, for UBSA, RBSA and RBAA, respectively (calculated based on the mass flow of the substance at the outlet). These suggest that variation of the building height enhances the canopy ventilation compared to a uniform height morphology, and staggered arrangement of the buildings slightly enhances the canopy ventilation compared to the aligned arrangement.

$$\overline{CW} = \bar{C}\overline{W} + \overline{C'W'} \qquad (1)$$

The flow regime over aligned uniform buildings – the case for most studies presented in the literature – has the same flow structure as that described by Oke (1988) as skimming flow, in which the vertical scalar transfer over an array of uniform height buildings is dominated by the turbulent component of the vertical flux. However, for staggered uniform arrays the flow regime is similar to that described by Oke (1988) as an isolated roughness flow. In this case (Figure 5), the vertical scalar transfer over an array of uniform height buildings contains significant turbulent and advective fractions of the vertical flux. The advective vertical scalar flux is negative at locations where the vertical component of the velocity is negative and it is responsible for enhancing the concentration within the canopy. While the turbulent vertical scalar flux is always positive and it is responsible for reducing the concentration within the canopy. The turbulent scalar flux for the positions measured just behind the building decreases its importance leaving the area source. This may be due to the fact that, away from the area source, the plume is more mixed and there is less scalar flux. It is important to note that some points are missing due to numerical error. In both cases the value of the turbulent and the advective scalar fluxes are similar leading to a total scalar fluxes near to zero.

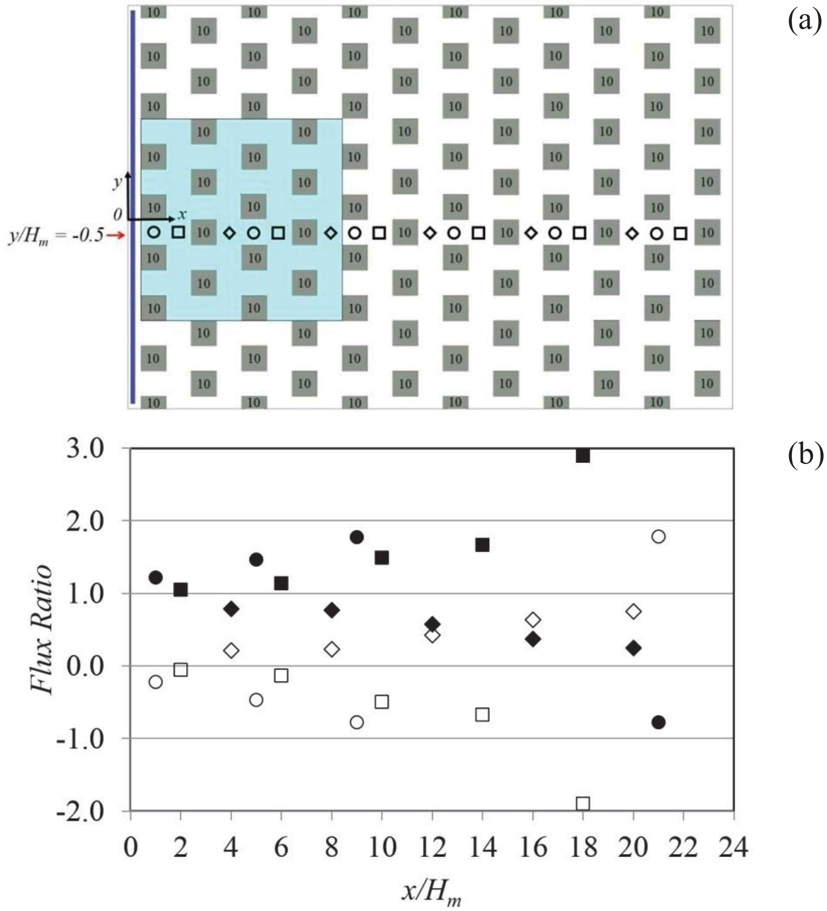

Figure 5. (a) Plan view of the UBSA and the sample locations, (b) ratio of advective scalar flux to total vertical flux (open symbols), and ratio of turbulent scalar fluxes to total vertical flux (solid symbols) calculated at y/H_m = -0.5.

In contrast, for the RBSA configuration (Figure 7), the advective component of the vertical flux becomes increasingly important for the determination of the total vertical scalar transfer. Fuka et al. (2017) show results from an LES simulation in which a tall building was placed within an array with uniform building height. They found that the taller building can significantly enhance or reduce the magnitude of the local scalar vertical flux, due to a significant alteration of the mean velocity field near the tall buildings, which contributes to an increased advective vertical flux bringing "cleaner" air from the upper atmosphere or contributing to a more intense exfiltration of the pollutants from the urban canopy.

Distribution of the normalized mean vertical velocity and its fluctuation in vertical planes along the array are presented in Figure 6 for all configurations. The main general structures that can be noticed are the stronger down and up drafts in front of and behind the tall buildings, respectively, for random heights configurations. Note also that the taller buildings promote an increase in the turbulent fluctuations of the vertical velocity above the smaller buildings. While the effects related to the mean flow are more local (close to the tall building), the effects related to the vertical velocity fluctuations, and consequentially the turbulent vertical fluxes, seem more largely spread downwind above the smaller buildings (non-local effect). In fact, it is clear that the increase in the turbulent fluctuations of the vertical velocity due to the presence of a tall building can be observed above smaller building as far as $7H_m$ downwind (Figures 6b and d).

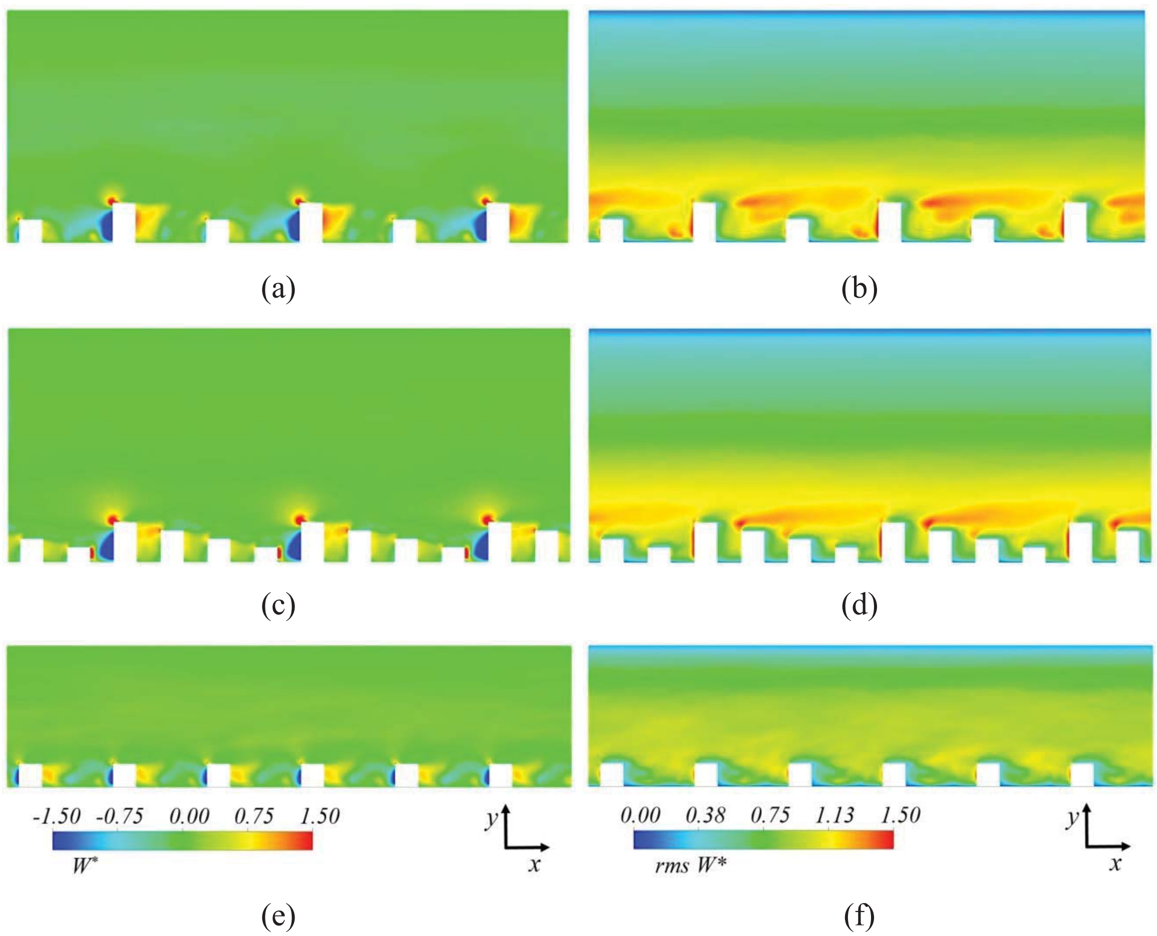

Figure 6. Distribution of normalized mean vertical velocity $(W^* = W/u_*)$ and $rms\ W^*$ on longitudinal planes located at y/H_m = -1.5 for (a) and (b) RBSA, (c) and (d) RBAA and (e) and (f) UBSA, respectively.

Analysing the effect of building height, it is possible to divide the pattern of vertical scalar flux in three difference groups resulting from morphologies where: (*i*) at least one building is lower than the average height as at y/H_m = -3.5 (Figure 7b); (*ii*) at least one building is taller than the array average height as at y/H_m = -1.5 (Figure 7c); and (*iii*) one building taller and one lower than the average height as at y/H_m = 0.5 (Figure 7d).

If (case i) the incoming flow passes over a low ($0.28H_m$) and an average height building (Figure 7b), the vertical scalar flux has the same pattern as the flow over a uniform height array of buildings. The vertical scalar flux is dominated by turbulence. If (case ii) the incoming flow passes over a series of buildings with one taller building ($1.72H_m$) (Figure 7c), the flow is disturbed by its presence and the advective part of the vertical scalar flux is significant. An intermediate pattern is found if (case iii) the sequence of buildings has buildings with lower and higher heights than the average (Figure 7d).

Analysing the aligned array (RBAA, Figure 8), one can find the same pattern but with smaller magnitude than the RBSA configuration (Figure 7). Since the aligned array produces more channelled flow than the staggered array, less vertical transport is expected. However, for the uniform height array (UBSA, Figure 5), the mean vertical velocity has a smaller magnitude compared with both arrays of random height building (RBSA and RBAA). It seems that tall buildings or an array of tall buildings enhance turbulence and therefore, the turbulent fluxes. The intensity of the effects of the turbulent structures seems to be related to the buildings height variation. The higher the buildings, the higher is the layer at which the flow has a larger turbulent velocity fluctuation.

Figure 8 presents the advective and turbulent vertical scalar fluxes calculated at $z/H_m = 1.0$ for the RBAA configuration at two different longitudinal (*x*-*z*) planes, one along a main street or canyon y/H_m = -0.5 (Figure 8b) and the other along a street crossing the buildings y/H_m = 0.5 (Figure 8c). Along the main street y/H_m = -0.5 the turbulent vertical scalar flux dominates. At y/H_m = 0.5 (Figure 8c), one can note a pattern of the advective flux fraction increasing and decreasing successively. This happens because of the sequence of increasing and decreasing building heights for this location. As a rule, the advective scalar flux dominates over turbulent scalar flux at the rear of the tallest building. Then, it decreases its importance as the turbulent scalar flux starts to increase. At the rear of the tallest building the turbulent vertical scalar flux reaches its minimum value and its maximum occurs between two buildings with the same height.

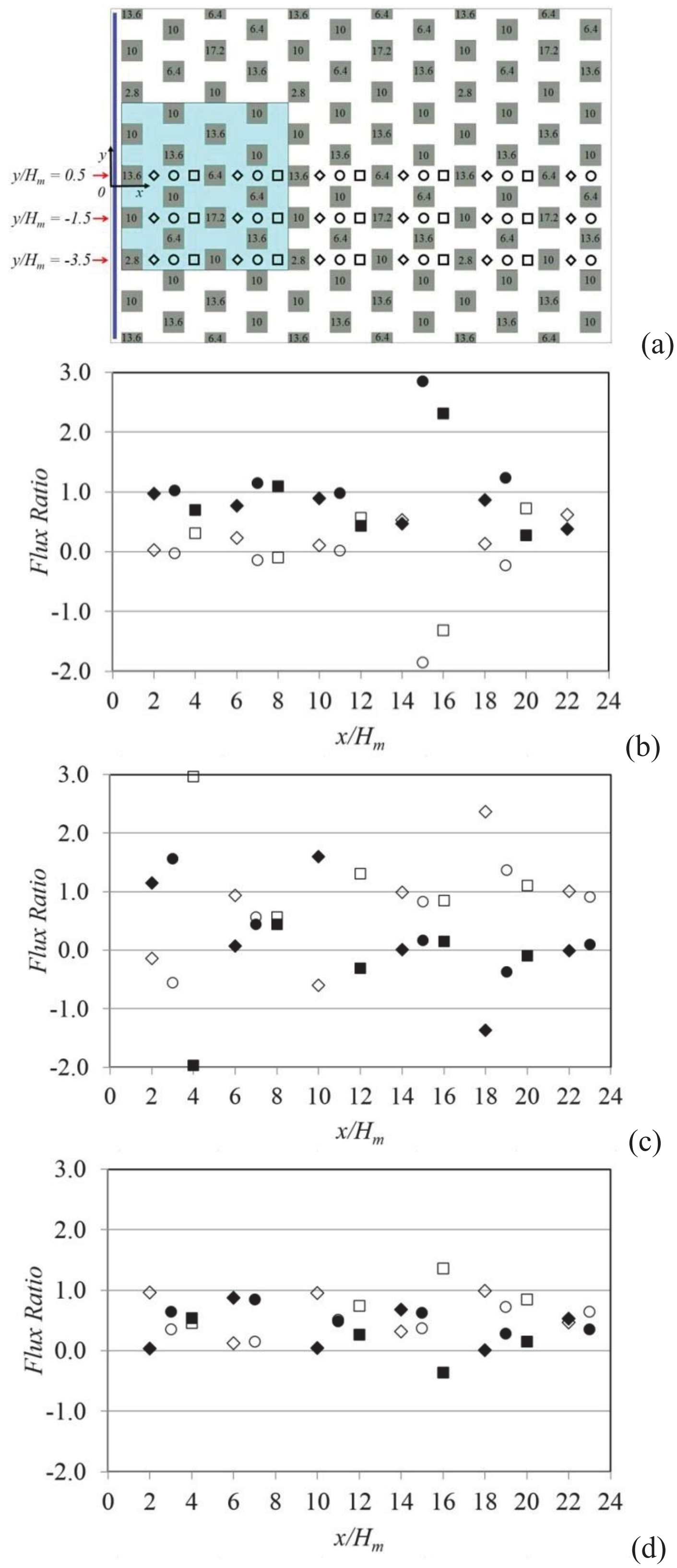

Figure 7. (a) Plan view of the RBSA and location of measurements. Ratio of advective scalar flux to total vertical flux (open symbols), and ratio of turbulent scalar fluxes to

total vertical flux (solid symbols) calculated at (b) y/H_m = -3.5, (c) y/H_m = -1.5 and (d) $y/H_m = 0.5$.

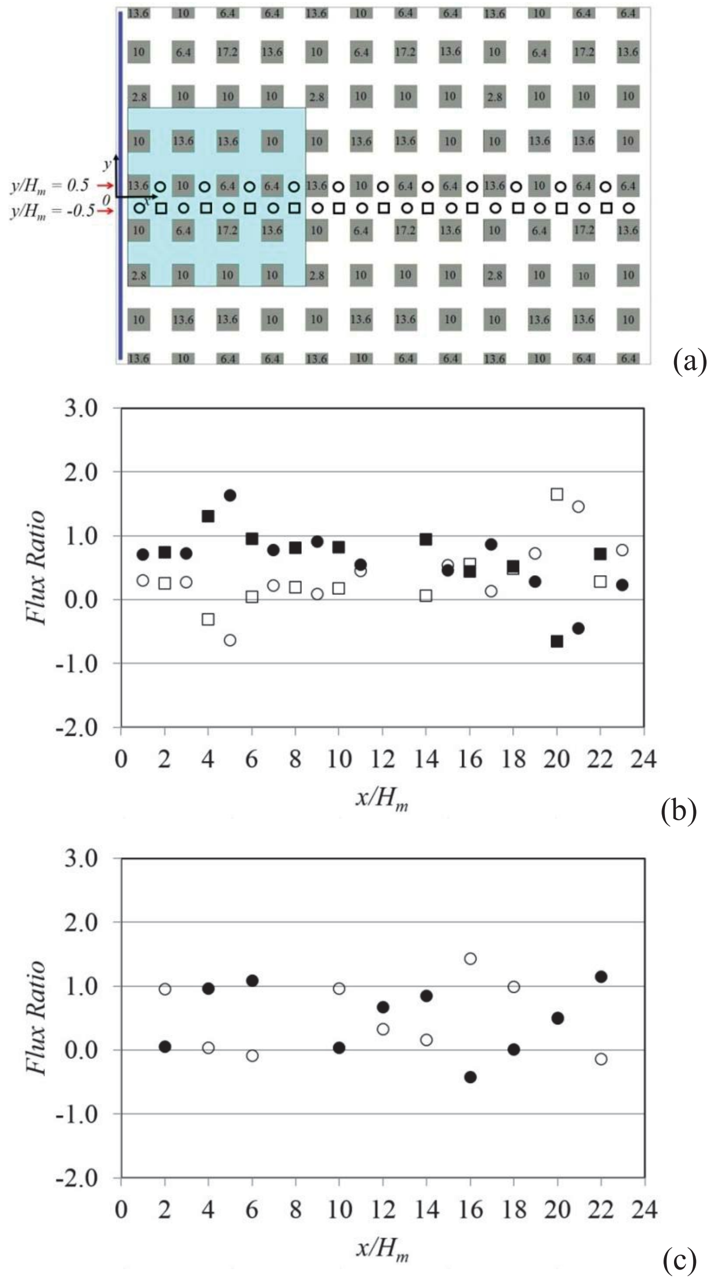

Figure 8. (a) Plan view of the RBAA and location of measurements. Ratio of advective scalar flux to total vertical flux (open symbols), and ratio of turbulent scalar fluxes to total vertical flux (solid symbols) for the RBAA calculated at (b) y/H_m = -0.5 and (c) $y/H_m = 0.5$.

3.3. Transport between urban areas downwind the emissions

The transport mechanisms outlined in the previous section affect significantly the pattern of transport between urban areas downwind of the emissions. The ratio of horizontal fluxes inside the canopy to the vertical flux to the atmosphere above is very important in determining the pollutant concentration in downwind areas.

Figure 9 shows vertical scalar fluxes (total, advective and turbulent) on a horizontal plane located at $z/H_m = 1.0$. Due to the larger concentrations close to the source, vertical fluxes are larger in this region. It is interesting to note that all three configurations (RBSA, RBAA, UBSA) exhibit regions with positive and negative local advective vertical scalar fluxes (Figures 9b, e and h). For the aligned configuration (with random building heights) the contribution of the advective vertical flux is due to the presence of the taller building. It is clear that close to the taller buildings the advective vertical flux is enhanced and close to short buildings its importance is reduced.

For the UBSA configuration (Figure 9h), the regions with positive and negative advective vertical flux are clearly marked. This is due to the flow regime over an staggered array where there are updraft and downdraft. For the RBSA the regions with positive and negative local advective vertical scalar fluxes can be explained as a combination form these two mechanisms, the urban configuration and the presence of tall buildings. Therefore, the advective vertical flux presents the largest value in the RBSA configuration.

Although there are patches of locally negative and positive fluxes, it is helpfull to investigate the average effect of the urban configuration upon the fluxes in the regions downwind of the source. In this sense, to investigate the effect that an emission in one urban zone would promote in a more distant clean zone (i.e. an urban area without any pollutant emission), we divided the simulation domain into three repeating units, as seen in Figure 1.

Spatially averaged vertical profiles of total, advective and turbulent non-dimensional scalar fluxes were calculated for the three different urban configurations (Figure 10).

Vertical scalar fluxes were spatially averaged over each urban zone every $0.2H_m$ from the ground until $4H_m$ to produce a vertical profile. As a general pattern, the total vertical scalar flux decreases with height above a certain height which is different depending on the urban zone (A, B or C) and the urban configuration. In zones B and C, the advective fluxes are very small (near to zero) compared to the turbulent fluxes at all heights for all configurations, being a little more important for configuration RBAA. In zone A, for all configurations, the total flux decreases with height. On the other hand, the partition between turbulent and advective vertical scalar flux is not similar for all configurations.

The advective vertical scalar flux in urban zone A within the canopy is smaller than the turbulent flux for the RBAA configuration as the unobstructed streets lead to a smaller magnitude of the vertical velocity component. It is important to remember that the tallest building for the random building configurations is 1.72 H_m and 1.0 H_m for the uniform building configuration. The advective scalar flux vanishes at a little above 1.0 H_m for all configurations. Above this height, the vertical scalar flux is dominated by turbulence. For urban zones B and C, the advective flux is negligible with values close to zero along the vertical direction.

In urban zone A for all configurations, the turbulent vertical scalar flux decreases rapidly with height until about $0.25H_m$ (Figures 10a, d and g). For the RBAA configuration (Figure 10d), it continues to decrease but more slowly, reaching a minimum at $2.5H_m$; the flow field is more structured with less blocking and, therefore, there is less turbulence and the turbulent scalar flux if smaller compared with the staggered configurations. For the UBSA configuration (Figure 10g), the turbulent vertical scalar flux continues to decrease until $0.25H_m$ then increases up to $1.0H_m$ before following the trend of dropping to a minimum close to $3.0H_m$. For the RBSA configuration (Figure 10a), the turbulent vertical scalar flux also decreases until $0.25H_m$ and then it is constant with height up to $1.0H_m$, subsequently decreasing slowly with height, reaching a minimum at $3.0H_m$.

For urban zones B (Figures 10b, e and h) and C (Figures 10c, f and i) , in all configurations the turbulent flux dominates over the advective flux with the advective scalar flux close to zero. Within the canopy the total vertical scalar flux increases with height for all simulations. For the staggered cases it increases linearly (Figures 10b and h) and for the aligned case (Figure 10e) the vertical profile increases slowly with height. However, for all simulations the peak of the vertical scalar flux is above the average building height. Increasing the distance from the source, the total vertical scalar flux is reduced and the maximum value is shifted upwards. Although the local advective vertical scalar flux is important near the vicinity of the tall buildings (Figures 5, 7 and 8), the spatially averaged vertical scalar flux indicates that the turbulent flux is dominant. The local advective vertical scalar flux close to tall buildings is important in setting the local concentration.

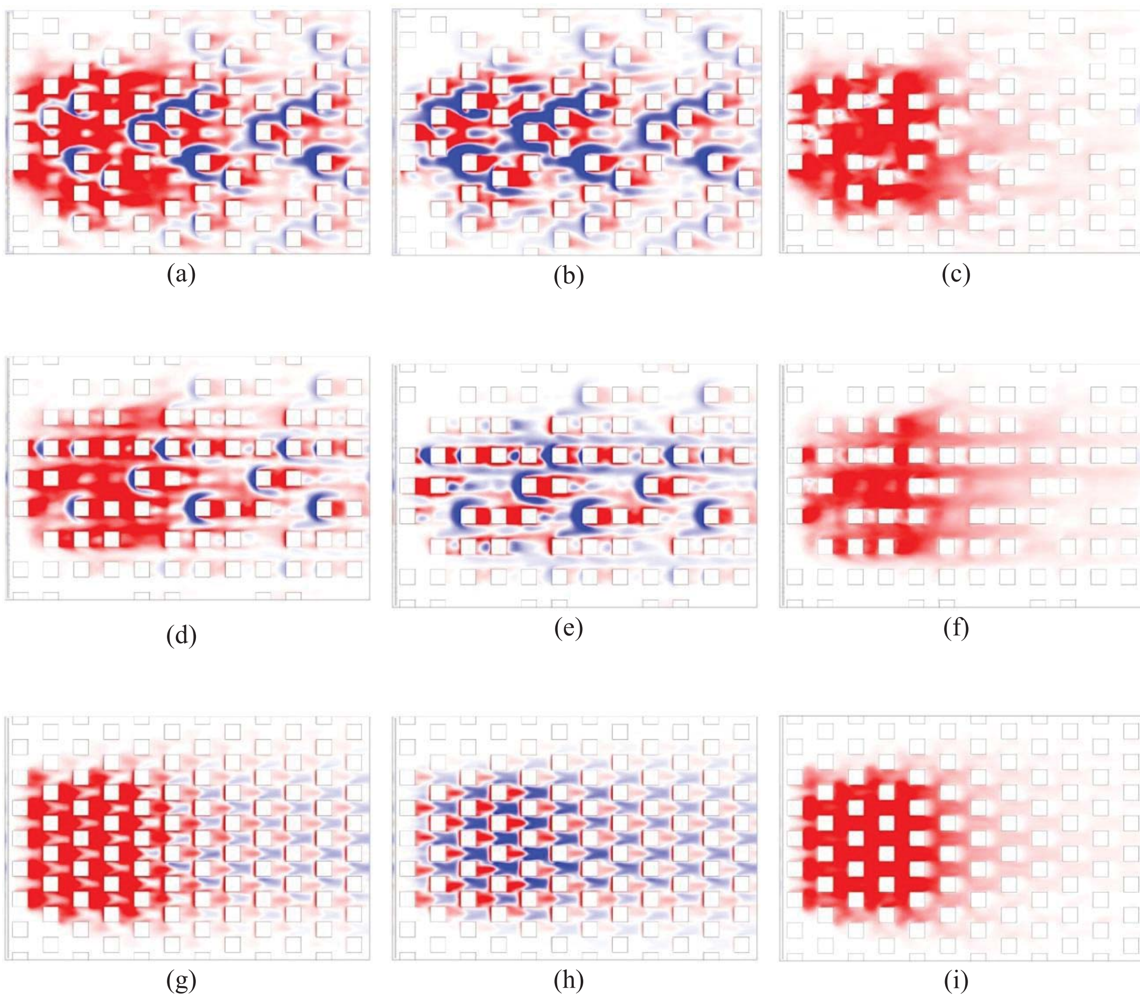

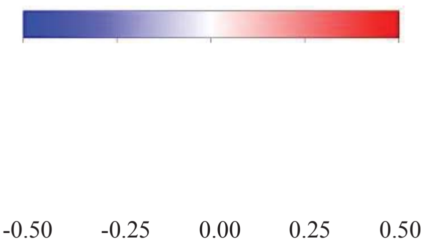

Figure 9. Vertical scalar fluxes on a horizontal plane located at $z/H_m = 1.0$: (a) total, (b) advective and (c) turbulent for RBSA, (d) total, (e) advective and (f) turbulent for RBAA and (g) total, (h) advective and (i) turbulent for UBSA, respectively.

It is important to note that the majority of street network dispersion models use the spatially averaged turbulent vertical scalar flux to parameterize the transfer velocity (Hertwig et al. 2018). However, this study suggests that it is inconsistent to estimate the transfer velocity assuming that the advective flux is negligible in the case of non-uniform building heights and non-aligned arrays.

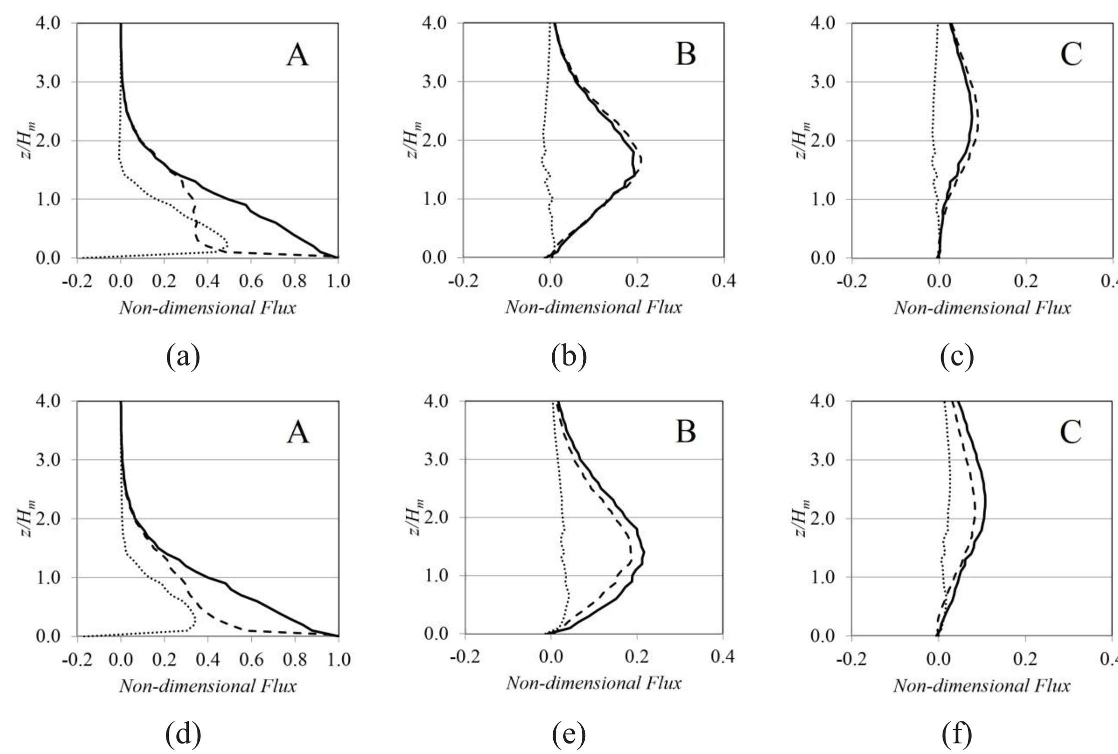

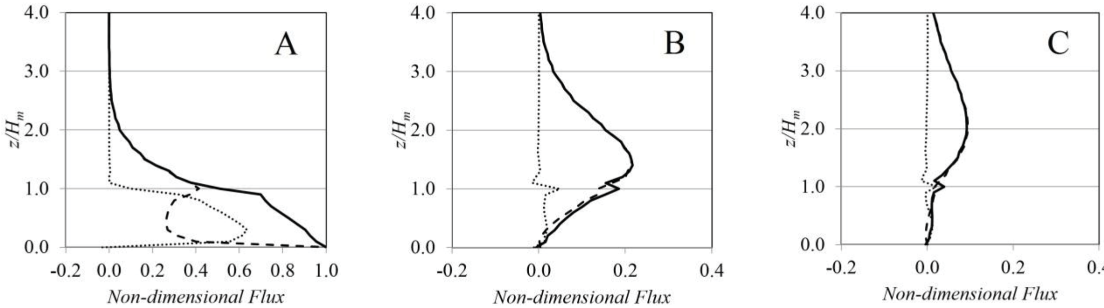

(g) (h) (i)

Figure 10. Spatially averaged vertical profiles of non-dimensional vertical scalar flux for the RBSA (a,b,c), RBAA (d,e,f), and UBSA (g,h,i) configurations,.Solid lines represent the total scalar flux, broken lines represent the turbulent scalar flux and dotted lines represents the advective scalar flux. Capital letters indicates the urban zones (see Figures 1b,d,f).

Therefore, the turbulent and advective vertical fluxes are very important inside the canopy over the area source; however, as the distance from the source increases the turbulent vertical flux dominates and is stronger above the canopy. This means that the pollutants emitted in the area source are well transported vertically by advection inside the canopy over the area source but are more strongly influenced by the turbulent flux above the canopy further from the source. Compared to the staggered configurations, it can also be seen that the vertical fluxes remain important inside the canopy for longer distances from the source for the RBAA due to the channelling effect.

Spatially averaged horizontal total, advective and turbulent scalar fluxes are presented in Figure 11 for the three urban zones in all configurations. Horizontal scalar fluxes were spatially averaged at the outlet of the urban zones over a line at every $0.2H_m$ from the ground until $4H_m$ to produce a vertical profile. While advective fluxes are the dominant mechanism responsible for horizontal transport, vertical transport results from a complex interaction between turbulent and advective fluxes, especially for the configuration with random building heights. Over the area source (zone A), for the staggered configurations (Figures 11a and g) there is an increase of the horizontal scalar flux with height because there is less obstruction to the flow. It reaches its peak at the canopy top and after that, the horizontal scalar flux decreases with height. In contrast, for the aligned configuration (Figure 11d), there is a decrease of the horizontal scalar flux with height, since there is less channeling of the flow with height. Note that the turbulent horizontal scalar flux is negative for the three cases in the three urban zones.

Figure 12 presents the ratio between vertical and averaged horizontal fluxes leaving zone A. The horizontal fluxes were averaged for two different vertical planes: from the ground to $z/H_m = 1.0$ and also to $z/H_m = 1.72$. As discussed previously, the proportion between horizontal fluxes inside the canopy and the vertical flux to the atmosphere above is very important in setting the pollutant concentration in downwind areas, since it will indicate the ratio between the amounts of pollutant transported from the canopy to the atmosphere above and the amount of pollutant transported to the region downwind. In general, the staggered configurations (RBSA and UBSA) yield a larger ratio between vertical and horizontal fluxes for $z/H_m = 1.0$, which indicates that these configurations have stronger vertical mass transfers than the aligned configuration. This trend is probably related to the channeling effect caused by the aligned streets in the RBAA configuration.

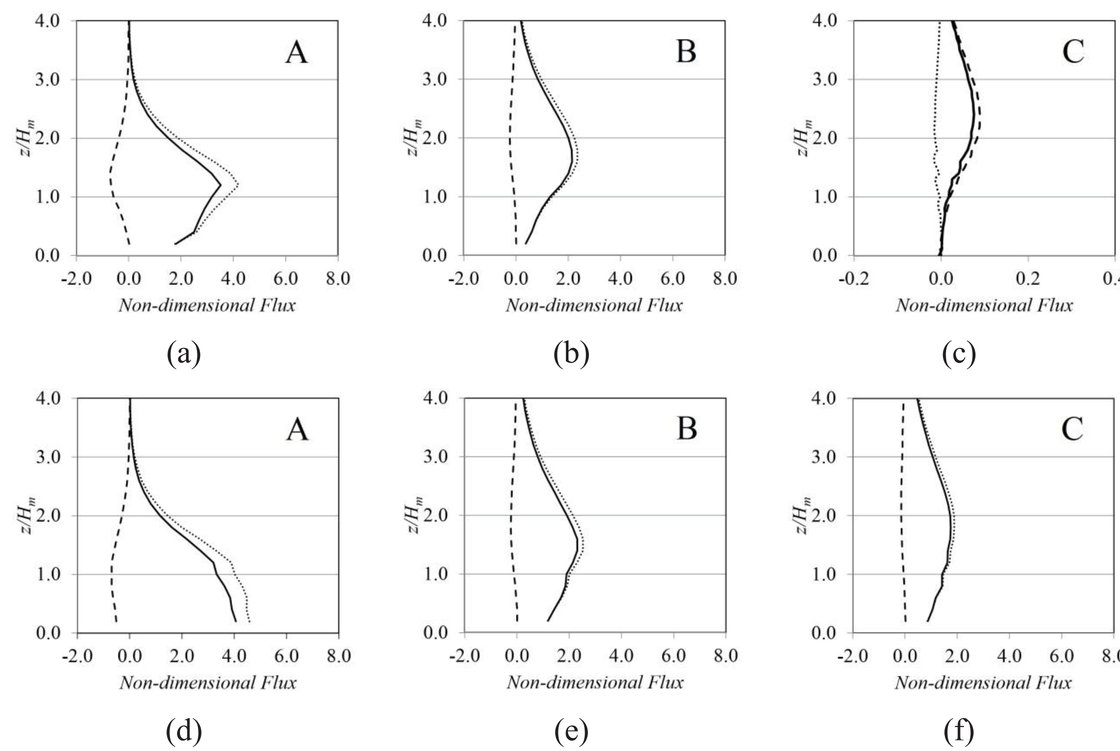

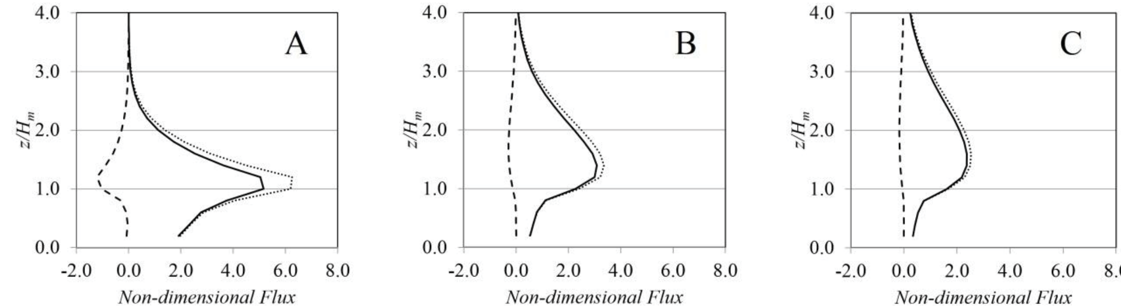

(g) (h) (i)

Figure 11. Spatially averaged vertical profile of horizontal scalar flux for RBSA (a,b,c) RBAA (d,e,f) and for UBSA (g,h,i) configurations. Solid lines represent the total scalar flux, broken lines represent the turbulent scalar flux and dotted lines represent the advective scalar flux. Capital letters indicates the urban zones (see Figure1b,d,f).

The configuration RBSA displays a ratio between vertical and horizontal fluxes larger than unity, which indicates that there is more mass leaving the canopy to the upper atmosphere than mass being transferred further downwind. The configuration UBSA also presents a ratio close to unity, but the value is more than 20% smaller than the value obtained for the RBSA configuration, which may indicate that random building heights play an important role in the process. For $z/H_m = 1.72$ a significant part of the scalar mass is still being transported upwards to the atmosphere in the cases with random building heights.

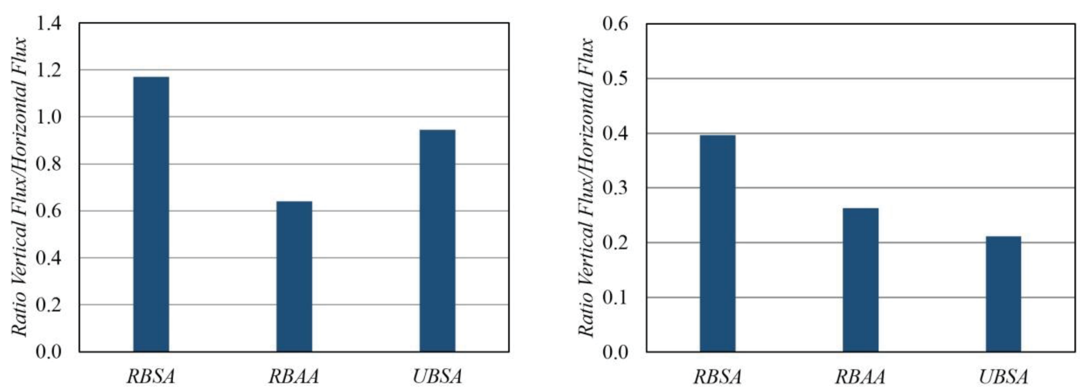

(a) (b)

Figure 12. Ratio between vertical and averaged horizontal fluxes leaving zone A, for (a) $z/H_m = 0$ to $z/H_m = 1.0$ and (b) $z/H_m = 0$ to $z/H_m = 1.72$.

4. Conclusions

The results demonstrate that the advective vertical scalar flux plays a very important role in the local transport of pollutants from/to the array, to an extent which varies according to building height differences and arrangements. In fact, in staggered array cases the advective vertical scalar flux has the same magnitude as the turbulent vertical scalar flux even in the case of uniform building heights. Moreover, the advective vertical scalar flux is negative in some locations, while the turbulent vertical scalar flux is always positive at all locations, enhancing and reducing, respectively, the concentration within the canopy.

In general, the staggered configurations (RBSA and UBSA) give a larger ratio between vertical and horizontal fluxes $at\ z/H_m = 1.0$, which indicates that these configurations yield stronger vertical mass transfer than the aligned configuration. This trend is probably related to the channeling effect caused by the aligned streets in the RBAA configuration.

For non-uniform heights arrays, there are intense down and up drafts in front of and behind the tall buildings. In addition, taller buildings promote an increase in the turbulent fluctuations of the vertical velocity above the smaller buildings. While the effects related to the mean flow are more local (close to the tall building), the effects related to the vertical velocity fluctuations, and consequentially the turbulent vertical fluxes, seem more largely spread downwind above the smaller buildings (a non-local effect).

It is important to highlight that although the local advective vertical scalar flux is important in the vicinity of the buildings, the spatially averaged vertical scalar flux indicates that the turbulent flux is dominant. Nonetheless, the local advective vertical scalar flux close to tall buildings remains important in determining the local concentration. This fact may prove to be a challenge for existing street network dispersion models that use the spatially average turbulent vertical scalar flux to parameterize the transfer velocity. Further research is needed on this topic.

Acknowledgements

This work was supported by the National Council for Scientific and Technological Development (CNPq) and Espírito Santo Research Foundation (FAPES) in Brazil and by the Newton Research Collaboration Programme Award NRCP1617-6-140, administered by the Royal Academy of Engineering as part of the UK Government's Newton Fund in UK. The first three authors acknowledge the hospitality provided by the Engineering Faculty of the University of Southampton during various extended visits as part of that Newton Fund support.

References

Aristodemou E, Boganegra LM, Mottet L, Pavlidis D, Constantinou A, Pain C, Robins A, ApSimon H. (2018) How tall buildings affect turbulent air flows and dispersion of pollution within a neighbourhood. Environmental Pollution, 233, 782-796

Boppana, V., Xie, Z.-T., and Castro, I. P. (2010). Large-eddy simulation of dispersion from surface sources in arrays of obstacles. Boundary layer meteorology, 135, 433-454.

Branford, S., Coceal, O., Thomas, T. G. and Belcher, S. E. (2011). Dispersion of a point-source release of a passive scalar through an urban-like array for different wind directions. Boundary Layer Meteorology, 363, 2947-2968.

Cai XM, Barlow JF, Belcher SE (2008) Dispersion and transfer of passive scalars in and above street canyons large-eddy simulations. Atmos Environ 42:5885–5895

Carpentieri, M., Robins, A. G. and Baldi, S. (2009). Three-dimensional mapping of air flow at an urban canyon intersection. Boundary Layer Meteorology, 133, 277-296.

Carpentieri, M., Robins, A. G., Hayden, P. and Santi, E. (2018). Mean and turbulent mass flux measurements in an idealised street network. Environmental Pollution, 234, 356-367.

Castro, I. P., Xie, Z.-T., V.Fuka, Robins, A. G., Carpentieri, M., Hayden, P., Hertwig, D. and Coceal, O. (2017). Measurements and computations of flow in an urban street system. Boundary Layer Meteorology, 162, 207-230.

Cheng, H. and Castro, I. P. (2002). Near wall ow over urban-like roughness. Boundary Layer Meteorology, 104, 229-259.

Coceal, O., Thomas, T. G., Castro, I. P. and Belcher, S. E. (2006). Mean flow and turbulent statistics over group of urban-like cubical obstacle. Boundary Layer Meteorology, 121, 491-519.

Coceal, O., Dobre, A., Thomas, T. G. and Belcher, S. E. (2007). Structure of turbulent flow over regular arrays of cubical roughness. Journal of Fluid Mechanics, 589, 375-409.

Coceal, O.; Goulart, E.V.; Branford, S.; Thomas, T.; Belcher, S.E, (2014). Flow structure and near-field dispersion in arrays of building-like obstacles. Journal of Wind Engineering and Industrial Aerodynamics, 125, 52-68

Davidson, M., Mylne, K.R., Jones, C.D., Phillips, J., Perkins, R.J., Jung, J. and Hunt, J. (1995). Plume dispersion through large groups of obstacles – a field investigation. Atmospheric Environment, 29, 3245-3256.

Fuka, V., Xie, Z.-T., Castro, I. P., Hayden, P., Carpentieri, M. and Robins, A. (2018). Scalar fluxes near a tall building in an aligned array of rectangular buildings. Boundary Layer Meteorology, 167, 103-124.

Goulart, E., Coceal, O., Branford, S., Thomas, T. G. and Belcher, S. (2016). Spatial and temporal variability of the concentration field from localized releases in a regular building array. Boundary-Layer Meteorology, 159, 241-257.

Goulart, E., Coceal, O. and Belcher, S. (2018). Dispersion of a passive scalar within and above an urban street network. Boundary-Layer Meteorology, 166, 241-257.

Hang J, Li YG. (2010) Ventilation strategy and air change rates in idealized high-rise compact urban areas. Building and Environment 45 (12): 2754-2767

Hang J, Li YG, Sandberg M. (2011) Experimental and numerical studies of flows through and within high-rise building arrays and their link to ventilation strategy. Journal of Wind Engineering and Industrial Aerodynamics, 99 (10): 1036-1055

J. Hang, Y. Li, M. Sandberg, R. Buccolieri, S. Di Sabatino, (2012) The influence of building height variability on pollutant dispersion and pedestrian ventilation in idealized high-rise urban areas, Building and Environment, 56, 346-360

Hertwig, D., Soulhac, L., Fuka, V.,Auerswald T., Carpentieri M., Hayden P., Robins A.G., Xie Z.T., Coceal O.. (2018) Evaluation of fast atmospheric dispersion models in a regular street network Environ. Fluid Mech..

Hilderman, T., Chong, R. and Kiel, D. (2004). Urban dispersion modelling data. Coanda Research and Development Corporation, 1, 1.

Kikumoto, H. and Ooka, R. (2018). Large-eddy simulation of pollutant dispersion in a cavity at fine grid resolutions. Building and Environment, 127, 127-137.

MacDonald, R., Grffiths, R.F. and Cheah, S.C. (1997). Field experiment of dispersion through regular array of cubic structure. Atmospheric Environment, 31, 783-795.

MacDonald, R., Griffiths, R. F. and Hall, D. J. (1998). A comparison of results from scaled field and wind tunnel modelling of dispersion in array of obstacles. Atmospheric Environment, 32, 3845-3862.

Pascheke, F., Barlow, J. and Robins, A. G. (2008). Wind-tunnel modelling of dispersion from a scalar area source in urban-like roughness. Boundary Layer Meteorology, 126, 103-124.

Phillips, D., Rossi, R. and Iaccarino, G. (2013). Large-eddy simulation of passive scalar dispersion in an urban-like canopy. Journal of Fluid Mechanics, 723, 404-428.

Smagorinsky, J. (1963) General circulation experiments with the primitive equations: I. The basic experiment. Monthly weather review, v. 91, n. 3, p. 99-164.

Tominaga, Y. and Stathopoulos, T. (2016). Ten questions concerning modelling of near-field pollutant dispersion in the built environment. Building and Environment, 105, 390-402.

Xie, Z.-T. and Castro, I. P. (2006). Les and rans for turbulent ow over arrays of wall-mounted obstacles. Flow Turbulence Combustion, 76, 291-312.

Xie, Z.-T., Coceal, O. and Castro, I. P. (2008). Large-eddy simulation of flows over random urban-like obstacles. Boundary Layer Meteorology, 129,1-23.

Xie ZT, Hayden P, Voke PR, Robins AG (2004) Large-eddy simulation of dispersion: comparison between elevated and ground-level sources. J*ournal of Turbulence* 5, 1–16

Yevgeny A. Gayev, Julian C.R. Hunt (2007). Flow and Transport Processes with Complex Obstructions: Applications to Cities, Vegetative Canopies and Industry. Springer Science & Business Media, Feb 6, 2007

Yoshida, T., Takemi, T., Horiguchi, M. (2018) Large-Eddy-Simulation Study of the Effects of Building-Height Variability on Turbulent Flows over an Actual Urban Area Boundary Layer Meteorology, 168, 127-153.

Yuan, C., Ng, E. and Norford, L. (2014). Improving air quality in high-density cities by understanding the relationship between air pollutant dispersion and urban morphologies. Building and Environment, 71, 245-258.

Zaki SA, Hagishima A, Tanimoto J, Ikegaya N (2011) Aerodynamic parameters of urban building arrays with random geometries. Boundary-Layer Meteorology 138(1), 99–120.

Title:

Local and non-local effects of building arrangements on pollutant fluxes within the urban canopy

Authors:

E V Goulart[1], N C Reis Jr[1], V F Lavor[1], Ian P Castro[2], J M Santos[1,*], Z. T. Xie[2]

Affiliations:

1. Department of Environmental Engineering, Universidade Federal do Espírito Santo, Brazil, Av. Fernando Ferrari 514, 29.075-910 Vitoria – ES, Brazil
2. Faculty of Engineering and the Environment, University of Southampton, Highfield, Southampton SO17 1BJ, UK

Abstract: This work investigates the vertical and horizontal mass (scalar) flux of a contaminant emitted from an area source located in an array of blocks representing an urban environment. Arrays consisting of buildings with random and uniform heights and staggered and aligned arrangements were tested. Results shows that the vertical scalar flux close to the source can affect downwind clean zones. It is also shown that taller buildings increase the vertical scalar flux and the fluctuations of the vertical velocity above the smaller buildings. The vertical advective scalar flux was found to have an effect on dispersion in the vicinity of the building (a local effect), while the vertical turbulent fluxes are associated with pollutant transportation downwind above the smaller buildings (a non-local effect).

Keywords: urban areas, dispersion, vertical scalar fluxes, random building height

1. Introduction

The wind flow over urban environments is affected by the geometrical features of buildings which in turn influence the vertical and horizontal fluxes of pollutants within the urban canopy and above. This influence can be seen locally in the vicinity of each building and also in the pollutants' transport from one region of the urban area to another further away.

Numerous experimental studies and numerical investigations have focused on understanding the wind flow and air pollutants dispersion affected by the presence of a buildings array which represents urban environments (Cheng and Castro, 2002; Coceal et al., 2006 and 2007; Xie et al., 2008; Pascheke et al., 2008; Boppana et al., 2010; Branford et al., 2011; Castro et al., 2017; Fuka et al., 2017; Kikumoto and Ooka, 2018; Carpentieri et al., 2018; among others). These can help urban planning for air quality improvement by supporting the choice of a more appropriate urban configuration in terms of the positioning of buildings and their three-dimensional characteristics (Yuan et al., 2014), or give support for building emergency plans in case of accidental or intentional releases of contaminants (Soulhac et al., 2011 and Soulhac et al., 2012).

The presence of buildings, especially tall buildings, disturbs the atmospheric flow considerably. Tominaga and Stathopoulos (2016) presented a review of near-field pollutant dispersion in built environments in which they explained the interaction between buildings and dispersion. Direct Numerical Simulation (DNS) of flow (Coceal et al., 2006 and 2007) and dispersion (Branford et al., 2011) of a passive pollutant emitted by a point source located within an array of cubic-like buildings revealed that the most significant processes controlling dispersion in urban areas are channelling flow along the streets, topological dispersion due to the presence of buildings (Branford et al 2011, Coceal et al 2014, Yevgeny et al 2007), plume skewing due to the flow turning with height, detrainment by turbulent dispersion, entrainment to building wakes, and development of secondary sources.

Recently, Goulart et al. (2017), using the same set of DNS data as Branford et al. (2011), investigated pollutant dispersion within and above the urban canopy. The results showed that the vertical pollutant mass (scalar) flux within the urban canopy is dominated by the turbulent component. On the other hand, the horizontal scalar flux below the canopy is dominated by advection while above the canopy there is a counter-gradient part of the turbulent horizontal scalar flux. As pointed out by Goulart et al. (2017), the vertical flux has an important role on how pollutants spreads through the array. Initial detrainment reduces pollutant concentration within the array. However, re-entrainment could increase concentration further away from the source.

Large Eddy Simulation (LES) has been used in numerical investigations of turbulent flow over an array of buildings. Xie et al. (2008), Fuka et al. (2017) and Castro et al. (2017) have shown that LES can yield excellent agreement with experimental and DNS data and therefore can be a reliable tool to investigate building-affected dispersion. Another recent example of LES reliability in modeling atmospheric turbulence in urban areas is the work of Yoshida et al. (2018) who used it to investigate the effects of building height variability on turbulent flows in the lower part of the urban boundary layer in Kyoto, comparing results to field experimental data. They showed that the plan-area index λ_p (the ratio of the plan area occupied by buildings to the total surface area) is an important parameter in distinguishing the effects of building height variability. A threshold for the influence of height randomness on turbulence variables become evident on flow and dispersion. It means that for sparsely populated (of buildings) sites, with $\lambda_p < 0.17$ according to Zaki *et al.* (2011), the height variability effects are not important. Our three simulated cases have $\lambda_p = 0.25$, so it is important to study the heights randomness effects.

A series of studies investigate how the high-rise building affects the flow and dispersion in pedestrian level. Aristodemou et al (20018) used wind tunnel and numerical simulation to investigate the effect of a tall building in flow and dispersion in a neighbourhood area. They found that the tall buildings affected the surrounding air flows and dispersion patterns, with the generation of “dead-zones” and high concentration “hotspots” in areas where these did not previously exist.

Hang and Li (2010) and Hang et al. (2011) investigated the flow and ventilation rates over array with high-rise building. They found that the ventilation rates decrease over arrays with tall buildings. While building height variation enhance vertical mean flows and therefore enhance the vertical ventilation in comparison to uniform buildings heights.

Hang et al (2012) studied pollutant dispersion over arrays with high-rise building. They found that, regarding pollutant removal, for canopies with the same average height (with different building height), the effects of turbulent diffusions are less important than the horizontal and vertical mean flow. They also pointed that as the standard deviation of the building heights increases, it lowers the pedestrian level concentration.

Fuka et al. (2017) used LES to investigate the fluid flow and dispersion of pollutants emitted from a ground point source within an array of buildings containing a tall one. They showed that the taller building significantly alters the flow field and can enhance or reduce the vertical scalar transfer depending on the location of the ground source relative to the tall building. These results agree with similar findings obtained by numerical simulations of wind flow over different urban configurations reported by Cheng and Castro (2002) and Xie et al. (2008). This also agrees with the results obtained by Boppana et al. (2010) whose work presented results for dispersion from an area source located within urban configurations identical to those used by Cheng and Castro (2002), Xie et al. (2008) and Pascheke et al. (2008) and showed that the dispersion pattern for the random height configuration is more complex than for a uniform height array. These studies have clearly demonstrated that canopy ventilation is very much affected by the surface morphology.

Carpentieri et al. (2018) measured turbulent and advective scalar flux over two arrays of rectangular buildings in a wind tunnel. The first array consisted of uniform height buildings and the second contained buildings of different heights. They also found that advective horizontal scalar fluxes were dominant over the turbulent scalar flux. However, they concluded that the advective and turbulent vertical scalar fluxes have the same order of magnitude. Moreover, the presence of a taller and isolated building upwind of the measurement enhances the vertical scalar transfer but building height variability seems to have an insignificant effect on the vertical scalar transfer, although their plan-area index was $\lambda_p = 0.54$, much greater than the threshold 0.3 suggested by Yoshida et al. (2018).

Therefore, the main aim of this work consists of analyzing how urban configuration affects the advective and turbulent vertical and horizontal fluxes of pollutant. The analysis was conducted considering the effect of taller buildings on the fluxes in their vicinity (a local effect) and downwind above the smaller buildings (a non-local effect). The vertical fluxes in and out of the canopy as well as the horizontal fluxes can help to describe the influence of building height variability and arrangements on the pollutant dispersion. In addition, the partition between advective and turbulent fluxes can be used to determine the characteristic velocity responsible for transporting the pollutants from within the canopy to the boundary layer above. We performed numerical simulations using LES to investigate flow and dispersion in three different urban-like configurations (uniform and random buildings heights in staggered and aligned configurations) in which the source is distributed spatially on the floor.

2. Mathematical Modeling

Figure 1 presents the three configurations considered. The first is a staggered array with random building heights (RBSA) (Figure 1a). The second is an aligned array with random building heights (RBAA) (Figure 1b). Finally, the last configuration is a staggered array with uniform building height (UBSA) (Figure 1c). In both cases of random buildings, the building height distribution follows a Gaussian distribution ranging from 2.8mm to 17.2mm. The computational domain plan area is $24H_m$ x $16H_m$ along the streamwise and spanwise directions, respectively (H_m is the average building height equal to 10mm). To further explore the downwind effects of different building heights and arrangement, the domain length of $24H_m$ is greater than the previous studies of Boppana et al. (2010). Each repeating unit comprised an array of sixteen blocks ($8H_m$ by $8H_m$). Therefore, the domain is one repeating unit longer in the streamwise direction than that of Boppana et al. (2010). The height of the domain is $6H_m$ and $10H_m$ for the uniform and random heights configurations, respectively.

To validate the flow field, the numerical results were compared with the wind tunnel data obtained by Cheng and Castro (2002) and the LES simulations performed by Xie et al. (2008). To validate the concentration field, the numerical results were compared with the wind tunnel data obtained by Pascheke et al. (2008) and the LES simulation performed by Boppana et al. (2010).

Table 1. Characteristic parameters

Configuration	$Re_H = u_H H_m/\nu$	u_H (ms^{-1})	Friction velocity, u_* (ms^{-1})
RBSA	1860.53	1.322	0.571
UBSA	1897.58	1.349	0.442
RBAA	2709.69	1.926	0.571

The freestream flow direction was parallel to the buildings walls (zero degrees) and the Reynolds number is defined as $Re_H = u_H H_m/\upsilon$ where u_H is the domain-averaged velocity at the average building height. Values of Reynolds number and friction velocity are presented in Table 1. Xie and Castro (2006) performed a series of LES simulation over array of buildings with Re varying from 5x103 to 5 x106. They concludes that dependency of the Reynolds number is poor. The weak dependency can be explained because the turbulence production has a comparable scale as the roughness elements. Also, the surface drag is basically due to the pressure related to the shape of the obstacle.

The Reynolds number effect can be important for a wind tunnel size model if skin friction, or surface scalar flux, or surface heat transfer is of interest. This paper is not focused on these. It is to be noted that in this paper, except for the validation, all of the results are presented in dimensionless data normalized by the flux at the source, with a focus on the study on dispersion away from the area source but not in the immediate vicinity of the source. This is governed by the building size scale turbulence, and should not significantly dependent on the Reynolds number.

In the laboratory experiments, naphthalene was coated onto the ground surface of the first repeating units of $8H_m$ x $8H_m$ to represent the area source, see the light blue area in Figure 1. The molecular Schmidt number Sc of naphtalene was assumed to be 2.284, as used by Boppana et al (2010) and Pascheke et al. (2008). An area source in an urban environment could be identified as a small localized zone where accidental or deliberate releases of pollutants or toxic gases can occur or perhaps a zone of heavy vehicle traffic.

Large-eddy simulation was used to simulate incompressible flow with ρ=1.225 kg m^{-3} and $\mu = 8.71\times10^{-6}$ kg m^{-1}s^{-1}. The Smagorinsky-Lilly model, which has a near-wall dumping function, with C_S = 0.1 was used to handle Subgrid scales, with the SGS turbulent Schmidt number taken as Sc_t =0.9 (Xie et al., 2004; Cai et al., 2008). Periodic boundary conditions were imposed in the main wind flow direction and on the lateral boundaries. Flow was maintained with a constant pressure gradient imposed in each control volume, given by $\partial P/\partial x = \rho u_*^2/L$ where u_* is the total wall friction velocity and L is the height of the domain. At all solid surfaces a no-slip boundary condition was applied. At the top of the domain, a free slip condition was applied. The area source was specified by a constant concentration equal to the saturation concentration of naphthalene in air (2x10^{-4} kg m^{-3}). A sponge layer (indicated as a blue line on Figure 1) was applied at the inlet to prevent pollutant mass from entering the domain.

The numerical simulations were performed using the commercial software Fluent Ansys version 18, which employs the finite volume method to discretize the conservation equations. A second order implicit scheme was chosen to discretize the temporal variables and a central differencing scheme was used for spatial discretization. Xie and Castro (2006) indicated that a mesh containing 16 cells over each cube dimension was adequate to simulate the flow past a staggered cube array, while Boppana et al. (2010) suggested that the accurate computation of the scalar fluxes close to the surface requires a much finer grid resolution. Based on grid checks, these authors indicated that a vertical cell size of H_m/64 close to the surface was required. Therefore, to optimize the cell size distribution, an eight million grid point hexahedral mesh was constructed with two mesh refinement regions. In the first region, 0 < z/H_m < 6, in order to accurately model the scalar fluxes close to the surface at the source location, a vertical cell size of H_m/75 resolution close to the surface was used, gradually expanding to H_m/16 (using a power-law), with a constant grid size of H_m/16 in the *x* and *y* directions. In the second region there was a step jump in mesh size , above z/H_m equal to 6, a uniform H_m/8 was used for all directions; since the main interest of this work is the prediction of the transport mechanism inside the building canopy this discontinuity in mesh size was not thought to be significant.

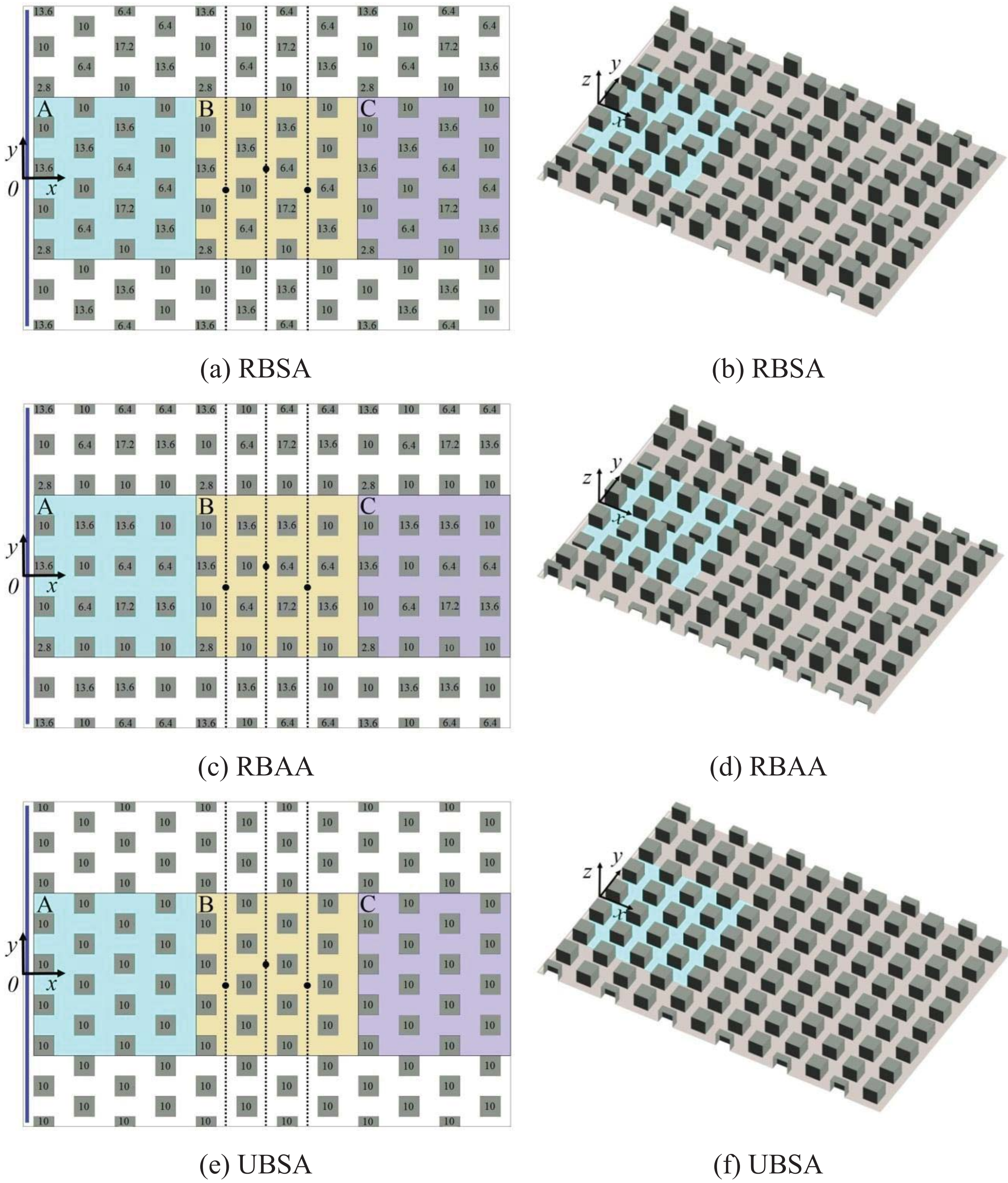

(a) RBSA (b) RBSA

(c) RBAA (d) RBAA

(e) UBSA (f) UBSA

Figure 1. (a), (c) & (e) are plan views of the urban configurations shown in (b), (d) & (f), respectively. The grey squares denote the building positions and the number inside each square denotes the building height in mm. The width in both streamwise and lateral directions of the buildings is 10 mm. The width of the streets is 10 mm. (a) staggered array with random buildings height (RBSA), (b) aligned array with random building height (RBAA) and (c) staggered array with uniform buildings height (UBSA). The regions marked with the capital letters A, B and C (in (a), (c), (e)) denote repeating units comprising sixteen blocks ($8H_m$ by $8H_m$), where the light blue zone (zone A)

coincide with the area source. Black dots show the locations of the vertical concentration profiles.

All simulations had a spin up period for flow and scalar field of at least $80T_C$ (characteristic time was defined as $T_C = H_m/u_*$). The time step for the simulations was $T_S = 0.002T_C$ and the total averaging time was at least $200T_C$ for all simulations.

3. Results and Discussion

The results are divided into three main parts. Firstly, Section 3.1 presents a comparison of the results obtained with previous wind tunnel experiments and LES simulations. Section 3.2 describes the local effects of building heights and arrangement upon the vertical flux of scalar. Finally, Section 3.3 explores the effect of emission over a downstream clean urban zone, discussing the local and non-local effects of the different configurations upon the vertical and streamwise component of the horizontal flux of scalar.

3.1. Comparison with a wind tunnel experiment and LES simulation

Spatially averaged streamwise velocities are presented in Figure 2. This Figure shows a comparison between the results obtained in the present work, the LES results obtained by Xie et al. (2008) and wind tunnel data obtained by Cheng and Castro (2002) for the staggered random height array configuration (RBSA) and the staggered uniform height array configuration (UBSA).

For the RBSA configuration, both LES simulations showed similar velocity profiles. Nevertheless, the velocity was underestimated at the top of the domain if compared with the wind tunnel data. The same result was found by Xie et al. (2008). Although, there are no wind tunnel data for the comparison of these variables in the UBSA configuration, we have chosen to present these results as they helpfully supplement the later comparison of concentration profiles for which wind tunnel data are available. The streamwise velocity profile indicates a stronger velocity gradient in the case of UBSA if compared with the RBSA configuration (Figure 2), which is perhaps not surprising.

Lateral and vertical profiles of concentration are presented for RBSA and UBSA configurations in Figures 3 and 4, respectively. Concentration is shown in non-dimensional form to enable comparison with results from previous works ($C^* = c/c_o$ where c_o is the concentration at the source). It can be seen that the LES results obtained in the present work show good agreement with LES results obtained by Boppana et al. (2010), as well as with experimental data obtained by Pascheke et al. (2008).

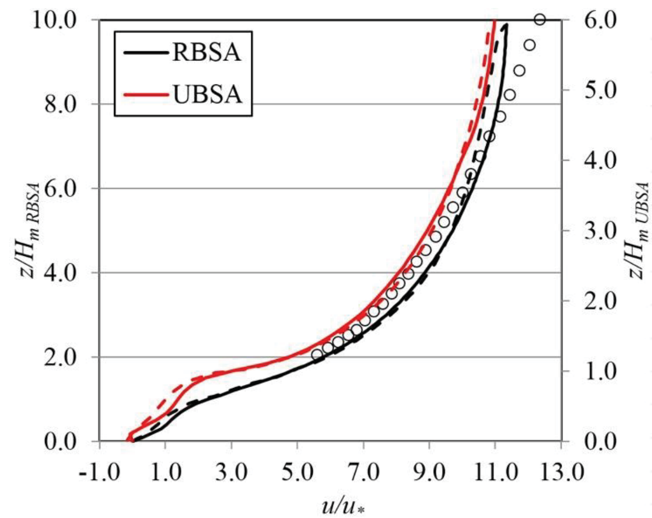

Figure 2. Spatially averaged mean velocity. Circles represent the wind tunnel velocity data obtained by Cheng and Castro (2002). Broken and solid lines indicate the LES velocity results produced by Xie et al. (2008) and in the present work, respectively.

For all configurations, concentrations are expected to decrease with distance from the source. However, for the RBSA configuration, there is a more three-dimensional flow with larger vertical scalar transfer and concentration is therefore expected to decrease more rapidly with distance as seen in Figure 3a. Further from the area source the lateral concentration profiles approach a Gaussian profile. Near the source, the effect of the buildings is more evident, modifying the lateral concentration profiles. For the RBSA configuration the profile showed in Figure 3a resembles a double-peak Gaussian profile due to the presence of a taller building (13.5 *mm*). Examining the uniform height array (UBSA), the concentration profile also approaches a Gaussian profile with distance from the source but does not present the double-peak feature (Figure 3). In this case (UBSA), the concentration peak is higher which indicates less vertical transfer.

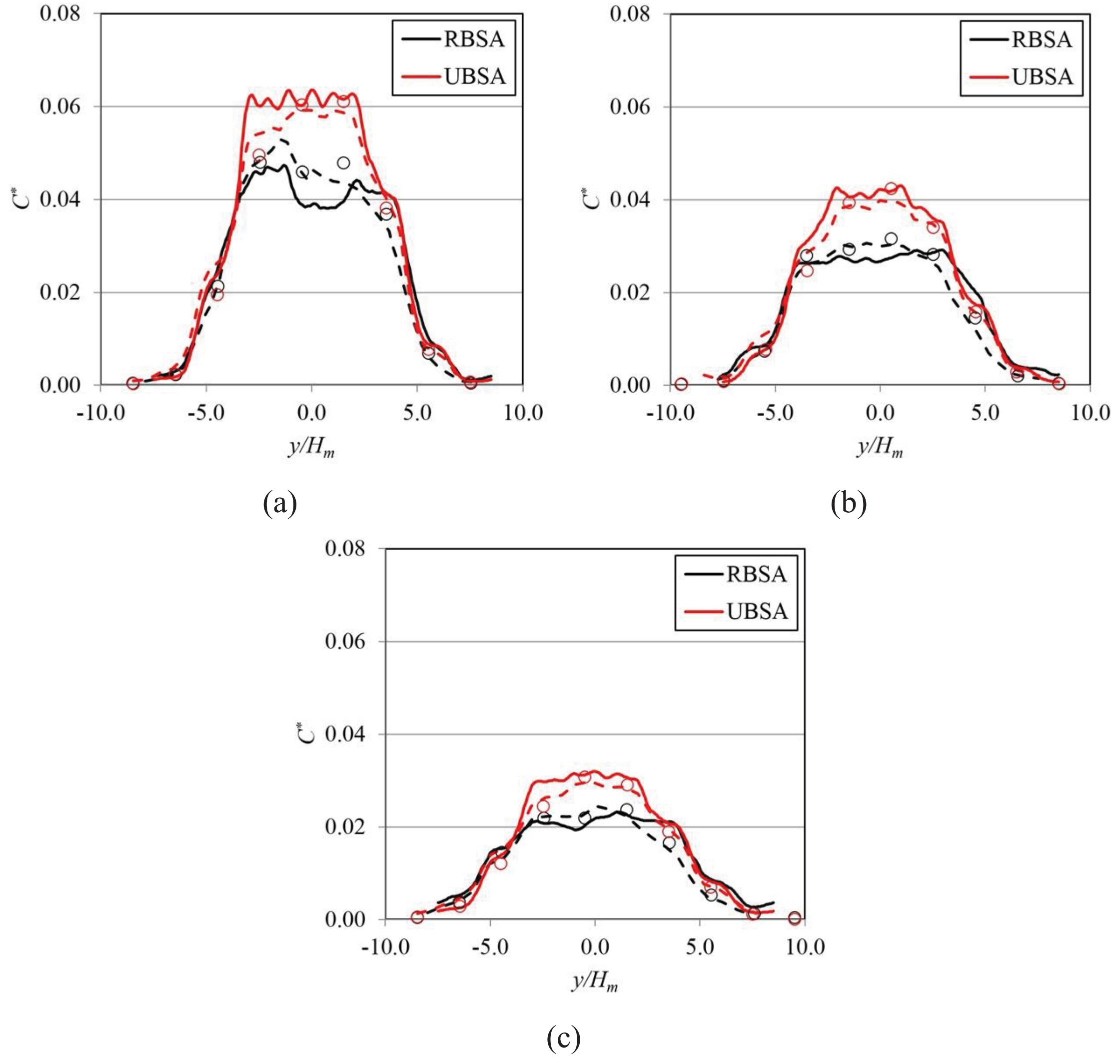

Figure 3. Lateral concentration profile for the RBSA and UBSA configurations calculated at $z/H_m = 0.6$ and three different downstream distances measured from the end of the area source: (a) $x/H_m = 10$, (b) $x/H_m = 12$ and (c) $x/H_m = 14$. Circles represent the wind tunnel concentration data obtained by Pascheke et al. (2008). Broken and solid lines indicate the LES concentration results produced by Boppana et al. (2010) and in the present work, respectively.

The vertical concentration gradient is steeper closer to the area source for all configurations. However, for the UBSA this gradient is even steeper than for the RBSA configuration. Branford et al. (2011) showed DNS results of the flow and dispersion of a ground point source over an array of uniform cubes and found little vertical exchange for cases in which wind direction is parallel to the array. Here, we found that the random building heights enhance the vertical scalar exchange. This is also supported by Castro et al. (2017) and Fuka et al. (2018). We will return to this point later.

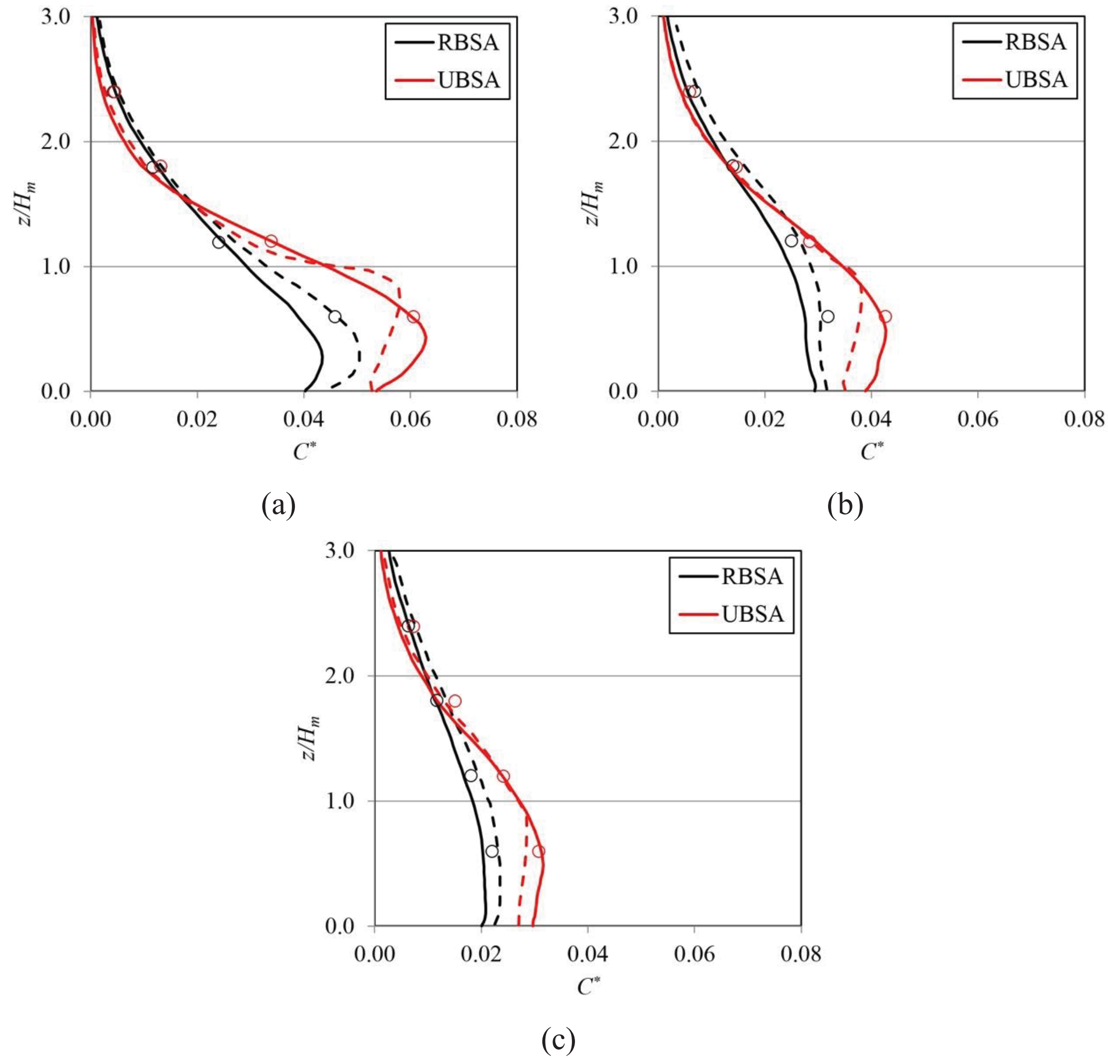

Figure 4. Vertical concentration profiles measured downstream the source area at (a) $x/H_m = 10$ and y/H_m= -0.5, (b) $x/H_m = 12$, y/H_m= 0.5 and (c) $x/H_m = 14$, y/H_m= -0.5 for the RBSA and UBSA configurations (black dots in Figure 1). Circles represent the wind tunnel concentration data obtained by Pascheke et al. (2008). Broken and solid lines indicate the LES concentration results produced by Boppana et al. (2010) and in the present work, respectively.

3.2 Local effect of pollutants fluxes on dispersion over an array of buildings

To explore the local effects of the differences in building heights on the scalar fluxes, spatially averaged vertical scalar fluxes were calculated as the average of the flux within a squared area at building height, comprising of Lx x Ly = 1H_m x 1H_m for all simulations as indicated in Equation 1, where the total scalar flux is the sum of the advective and turbulent vertical scalar fluxes. Partition of the turbulent and advective scalar fluxes normalized by the time-averaged scalar flux emitted by the source are presented in Figures 5, 7 and 8 for different lines along the array at z/H_m =1.0, for UBSA, RBSA and RBAA, respectively. The averaged scalar fluxes at the source were 6.27 x10^{-6} kg m^{-2} s^{-1}, 7.37x10^{-6} kg m^{-2} s^{-1} and 7.12 x10^{-6} kg m^{-2} s^{-1}, for UBSA, RBSA and RBAA, respectively (calculated based on the mass flow of the substance at the outlet). These suggest that variation of the building height enhances the canopy ventilation compared to a uniform height morphology, and staggered arrangement of the buildings slightly enhances the canopy ventilation compared to the aligned arrangement.

$$\overline{CW} = \bar{C}\overline{W} + \overline{C'W'} \qquad 1$$

The flow regime over aligned uniform buildings – the case for most studies presented in the literature – has the same flow structure as that described by Oke (1988) as skimming flow, in which the vertical scalar transfer over an array of uniform height buildings is dominated by the turbulent component of the vertical flux. However, for staggered uniform arrays the flow regime is similar to that described by Oke (1988) as an isolated roughness flow. In this case (Figure 5), the vertical scalar transfer over an array of uniform height buildings contains significant turbulent and advective fractions of the vertical flux. The advective vertical scalar flux is negative at locations where the vertical component of the velocity is negative and it is responsible for enhancing the concentration within the canopy. While the turbulent vertical scalar flux is always positive and it is responsible for reducing the concentration within the canopy. The turbulent scalar flux for the positions measured just behind the building decreases its importance leaving the area source. This may be due to the fact that, away from the area source, the plume is more mixed and there is less scalar flux. It is important to note that some points are missing due to numerical error. In both cases the value of the turbulent and the advective scalar fluxes are similar leading to a total scalar fluxes near to zero.

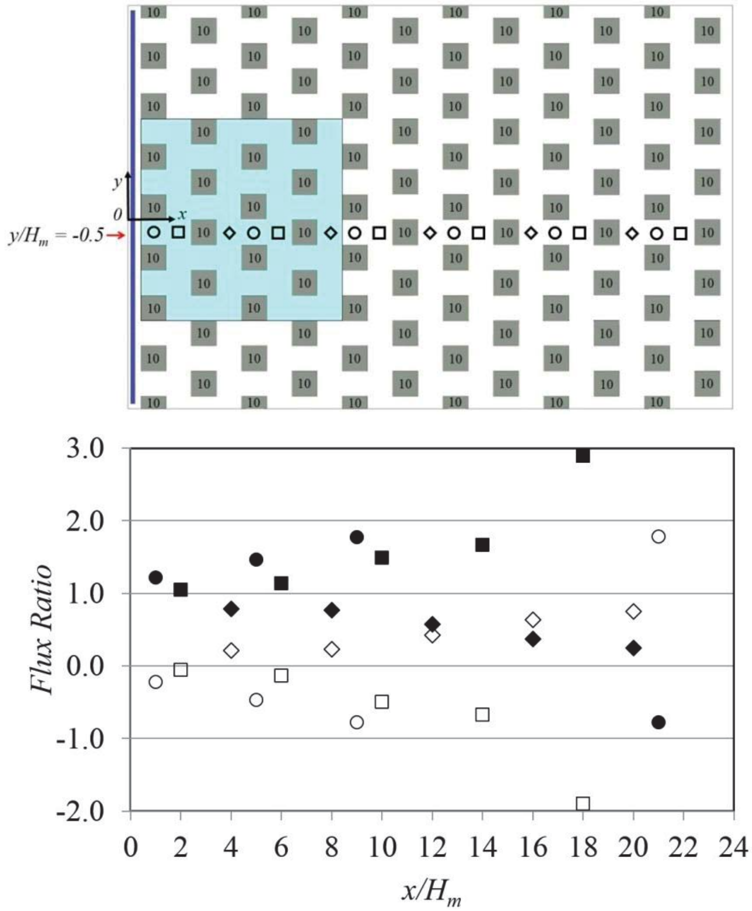

(a)

(b)

Figure 5. (a) Plan view of the UBSA and the sample locations, (b) ratio of advective scalar flux to total vertical flux (open symbols), and ratio of turbulent scalar fluxes to total vertical flux (solid symbols) calculated at y/H_m = -0.5.

In contrast, for the RBSA configuration (Figure 7), the advective component of the vertical flux becomes increasingly important for the determination of the total vertical scalar transfer. Fuka et al. (2017) show results from an LES simulation in which a tall building was placed within an array with uniform building height. They found that the taller building can significantly enhance or reduce the magnitude of the local scalar vertical flux, due to a significant alteration of the mean velocity field near the tall buildings, which contributes to an increased advective vertical flux bringing "cleaner" air from the upper atmosphere or contributing to a more intense exfiltration of the pollutants from the urban canopy.

Distribution of the normalized mean vertical velocity and its fluctuation in vertical planes along the array are presented in Figure 6 for all configurations. The main general structures that can be noticed are the stronger down and up drafts in front of and behind the tall buildings, respectively, for random heights configurations. Note also that the taller buildings promote an increase in the turbulent fluctuations of the vertical velocity above the smaller buildings. While the effects related to the mean flow are more local (close to the tall building), the effects related to the vertical velocity fluctuations, and consequentially the turbulent vertical fluxes, seem more largely spread downwind above the smaller buildings (non-local effect). In fact, it is clear that the increase in the turbulent fluctuations of the vertical velocity due to the presence of a tall building can be observed above smaller building as far as $7H_m$ downwind (Figures 6b and d).

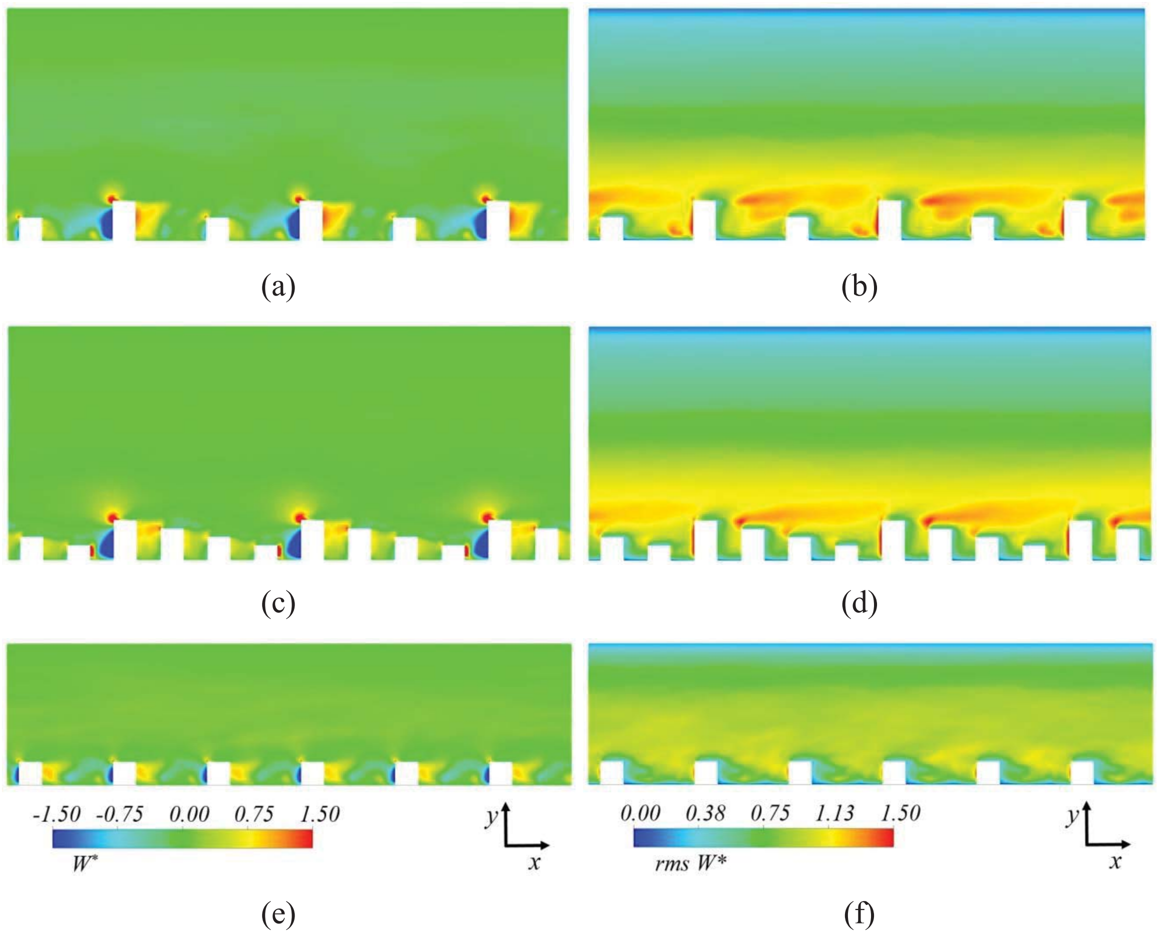

Figure 6. Distribution of normalized mean vertical velocity ($W^* = W/u_*$) and $rms\ W^*$ on longitudinal planes located at y/H_m = -1.5 for (a) and (b) RBSA, (c) and (d) RBAA and (e) and (f) UBSA, respectively.

Analysing the effect of building height, it is possible to divide the pattern of vertical scalar flux in three difference groups resulting from morphologies where: (i) at least one building is lower than the average height as at y/H_m = -3.5 (Figure 7b); (ii) at least one building is taller than the array average height as at y/H_m = -1.5 (Figure 7c); and (*iii*) one building taller and one lower than the average height as at y/H_m = 0.5 (Figure 7d).

If (case i) the incoming flow passes over a low ($0.28H_m$) and an average height building (Figure 7b), the vertical scalar flux has the same pattern as the flow over a uniform height array of buildings. The vertical scalar flux is dominated by turbulence. If (case ii) the incoming flow passes over a series of buildings with one taller building ($1.72H_m$) (Figure 7c), the flow is disturbed by its presence and the advective part of the vertical scalar flux is significant. An intermediate pattern is found if (case iii) the sequence of buildings has buildings with lower and higher heights than the average (Figure 7d).

Analysing the aligned array (RBAA, Figure 8), one can find the same pattern but with smaller magnitude than the RBSA configuration (Figure 7). Since the aligned array produces more channelled flow than the staggered array, less vertical transport is expected. However, for the uniform height array (UBSA, Figure 5), the mean vertical velocity has a smaller magnitude compared with both arrays of random height building (RBSA and RBAA). It seems that tall buildings or an array of tall buildings enhance turbulence and therefore, the turbulent fluxes. The intensity of the effects of the turbulent structures seems to be related to the buildings height variation. The higher the buildings, the higher is the layer at which the flow has a larger turbulent velocity fluctuation.

Figure 8 presents the advective and turbulent vertical scalar fluxes calculated at z/H_m = 1.0 for the RBAA configuration at two different longitudinal (*x*-*z*) planes, one along a main street or canyon y/H_m = -0.5 (Figure 8b) and the other along a street crossing the buildings y/H_m = 0.5 (Figure 8c). Along the main street y/H_m = -0.5 the turbulent vertical scalar flux dominates. At y/H_m = 0.5 (Figure 8c), one can note a pattern of the advective flux fraction increasing and decreasing successively. This happens because of the sequence of increasing and decreasing building heights for this location. As a rule, the advective scalar flux dominates over turbulent scalar flux at the rear of the tallest building. Then, it decreases its importance as the turbulent scalar flux starts to increase. At the rear of the tallest building the turbulent vertical scalar flux reaches its minimum value and its maximum occurs between two buildings with the same height.

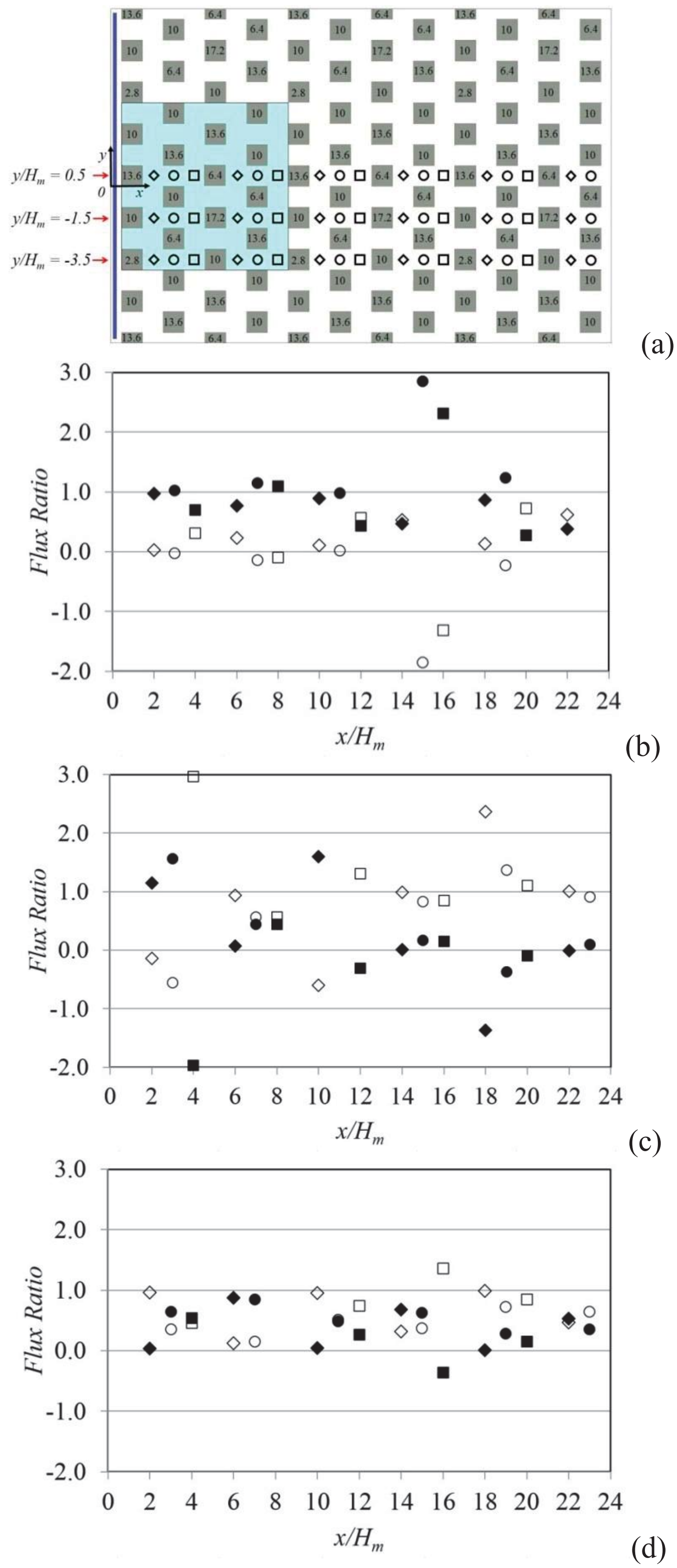

Figure 7. (a) Plan view of the RBSA and location of measurements. Ratio of advective scalar flux to total vertical flux (open symbols), and ratio of turbulent scalar fluxes to

total vertical flux (solid symbols) calculated at (b) y/H_m = -3.5, (c) y/H_m = -1.5 and (d) $y/H_m = 0.5$.

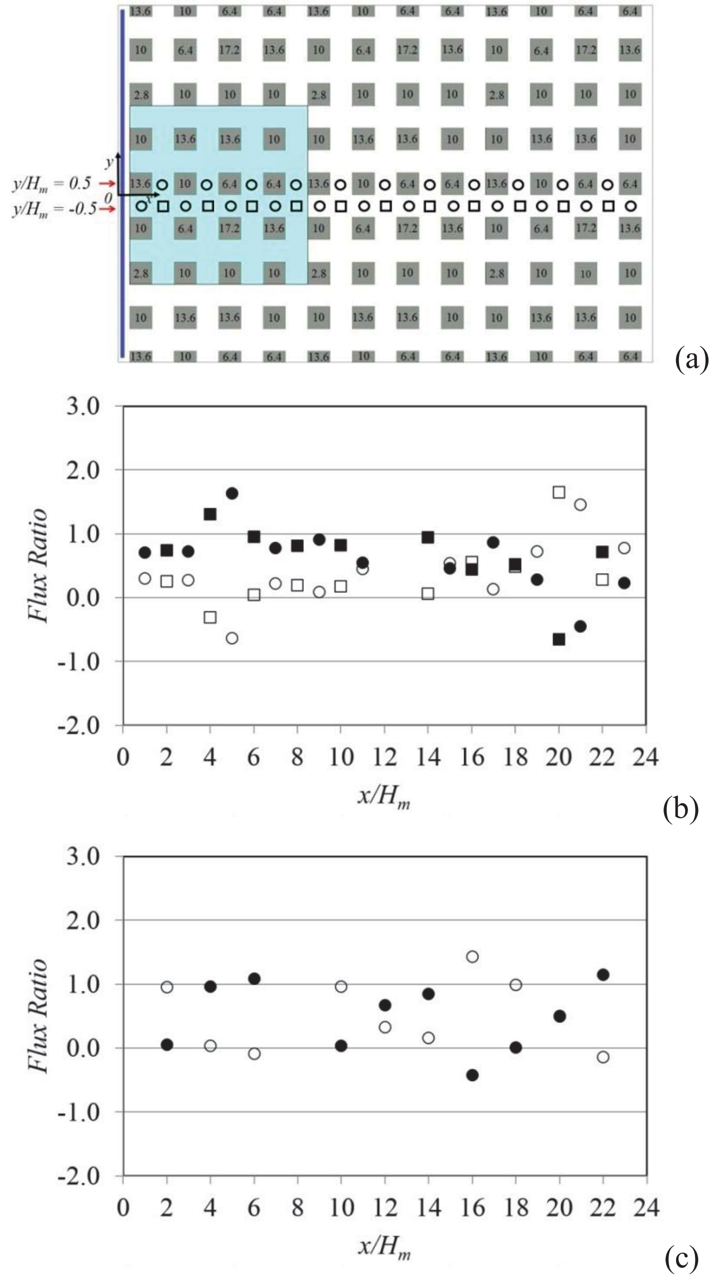

Figure 8. (a) Plan view of the RBAA and location of measurements. Ratio of advective scalar flux to total vertical flux (open symbols), and ratio of turbulent scalar fluxes to total vertical flux (solid symbols) for the RBAA calculated at (b) y/H_m = -0.5 and (c) $y/H_m = 0.5$.

3.3. Transport between urban areas downwind the emissions

The transport mechanisms outlined in the previous section affect significantly the pattern of transport between urban areas downwind of the emissions. The ratio of horizontal fluxes inside the canopy to the vertical flux to the atmosphere above is very important in determining the pollutant concentration in downwind areas.

Figure 9 shows vertical scalar fluxes (total, advective and turbulent) on a horizontal plane located at $z/H_m = 1.0$. Due to the larger concentrations close to the source, vertical fluxes are larger in this region. It is interesting to note that all three configurations (RBSA, RBAA, UBSA) exhibit regions with positive and negative local advective vertical scalar fluxes (Figures 9b, e and h). For the aligned configuration (with random building heights) the contribution of the advective vertical flux is due to the presence of the taller building. It is clear that close to the taller buildings the advective vertical flux is enhanced and close to short buildings its importance is reduced.

For the UBSA configuration (Figure 9h), the regions with positive and negative advective vertical flux are clearly marked. This is due to the flow regime over an staggered array where there are updraft and downdraft. For the RBSA the regions with positive and negative local advective vertical scalar fluxes can be explained as a combination form these two mechanisms, the urban configuration and the presence of tall buildings. Therefore, the advective vertical flux presents the largest value in the RBSA configuration.

Although there are patches of locally negative and positive fluxes, it is helpfull to investigate the average effect of the urban configuration upon the fluxes in the regions downwind of the source. In this sense, to investigate the effect that an emission in one urban zone would promote in a more distant clean zone (i.e. an urban area without any pollutant emission), we divided the simulation domain into three repeating units, as seen in Figure 1.

Spatially averaged vertical profiles of total, advective and turbulent non-dimensional scalar fluxes were calculated for the three different urban configurations (Figure 10).

Vertical scalar fluxes were spatially averaged over each urban zone every $0.2H_m$ from the ground until $4H_m$ to produce a vertical profile. As a general pattern, the total vertical scalar flux decreases with height above a certain height which is different depending on the urban zone (A, B or C) and the urban configuration. In zones B and C, the advective fluxes are very small (near to zero) compared to the turbulent fluxes at all heights for all configurations, being a little more important for configuration RBAA. In zone A, for all configurations, the total flux decreases with height. On the other hand, the partition between turbulent and advective vertical scalar flux is not similar for all configurations.

The advective vertical scalar flux in urban zone A within the canopy is smaller than the turbulent flux for the RBAA configuration as the unobstructed streets lead to a smaller magnitude of the vertical velocity component. It is important to remember that the tallest building for the random building configurations is 1.72 H_m and 1.0 H_m for the uniform building configuration. The advective scalar flux vanishes at a little above 1.0 H_m for all configurations. Above this height, the vertical scalar flux is dominated by turbulence. For urban zones B and C, the advective flux is negligible with values close to zero along the vertical direction.

In urban zone A for all configurations, the turbulent vertical scalar flux decreases rapidly with height until about $0.25H_m$ (Figures 10a, d and g). For the RBAA configuration (Figure 10d), it continues to decrease but more slowly, reaching a minimum at $2.5H_m$; the flow field is more structured with less blocking and, therefore, there is less turbulence and the turbulent scalar flux if smaller compared with the staggered configurations. For the UBSA configuration (Figure 10g), the turbulent vertical scalar flux continues to decrease until $0.25H_m$ then increases up to $1.0H_m$ before following the trend of dropping to a minimum close to $3.0H_m$. For the RBSA configuration (Figure 10a), the turbulent vertical scalar flux also decreases until $0.25H_m$ and then it is constant with height up to $1.0H_m$, subsequently decreasing slowly with height, reaching a minimum at $3.0H_m$.

For urban zones B (Figures 10b, e and h) and C (Figures 10c, f and i) , in all configurations the turbulent flux dominates over the advective flux with the advective scalar flux close to zero. Within the canopy the total vertical scalar flux increases with height for all simulations. For the staggered cases it increases linearly (Figures 10b and h) and for the aligned case (Figure 10e) the vertical profile increases slowly with height. However, for all simulations the peak of the vertical scalar flux is above the average building height. Increasing the distance from the source, the total vertical scalar flux is reduced and the maximum value is shifted upwards. Although the local advective vertical scalar flux is important near the vicinity of the tall buildings (Figures 5, 7 and 8), the spatially averaged vertical scalar flux indicates that the turbulent flux is dominant. The local advective vertical scalar flux close to tall buildings is important in setting the local concentration.

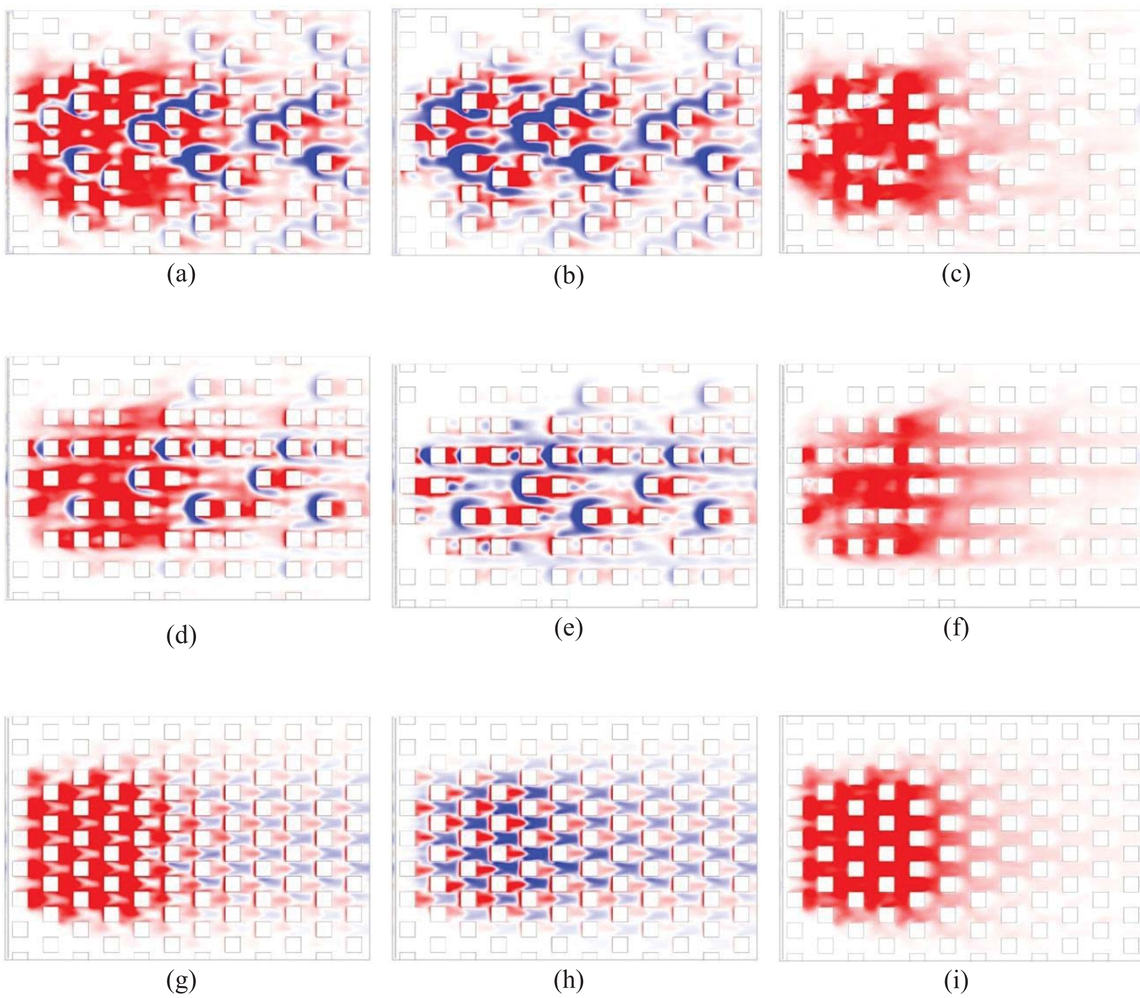

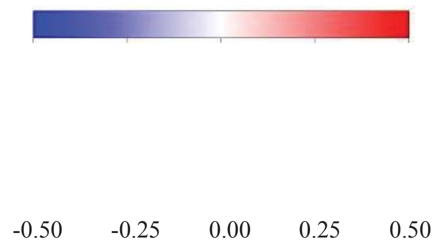

Figure 9. Vertical scalar fluxes on a horizontal plane located at $z/H_m = 1.0$: (a) total, (b) advective and (c) turbulent for RBSA, (d) total, (e) advective and (f) turbulent for RBAA and (g) total, (h) advective and (i) turbulent for UBSA, respectively.

It is important to note that the majority of street network dispersion models use the spatially averaged turbulent vertical scalar flux to parameterize the transfer velocity (Hertwig et al. 2018). However, this study suggests that it is inconsistent to estimate the transfer velocity assuming that the advective flux is negligible in the case of non-uniform building heights and non-aligned arrays.

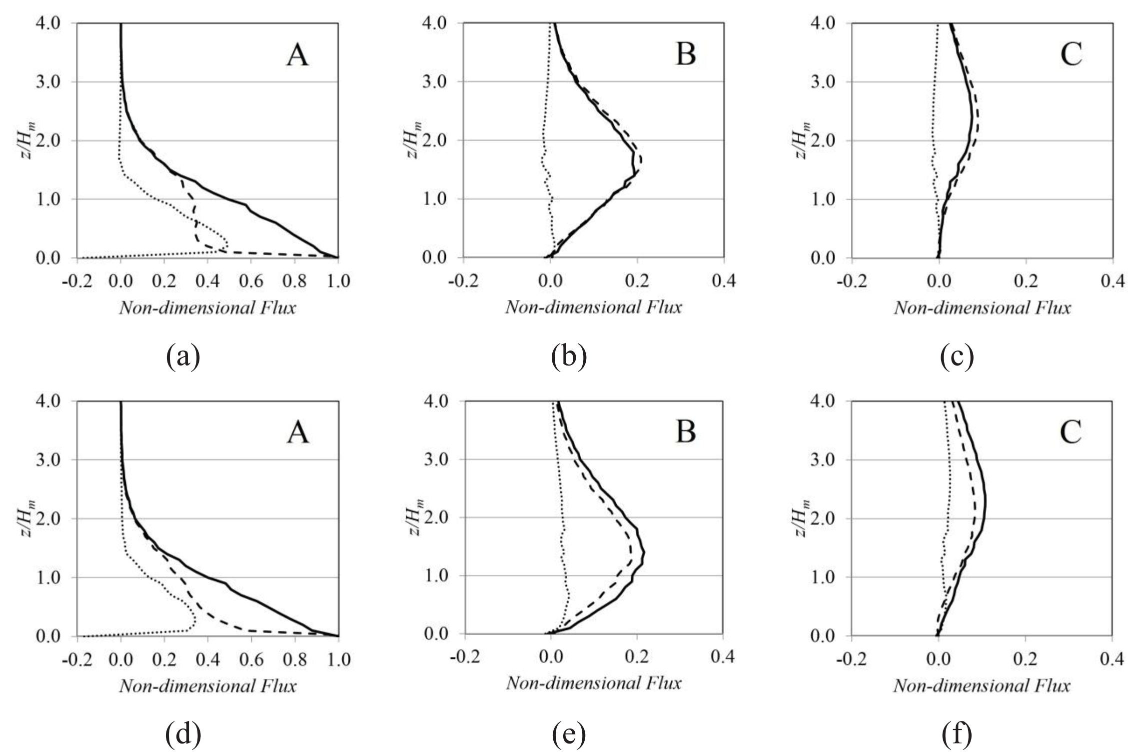

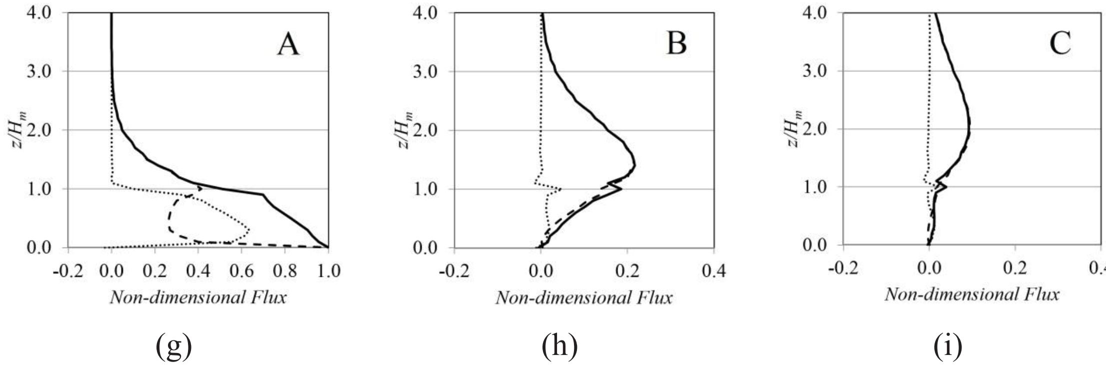

Figure 10. Spatially averaged vertical profiles of non-dimensional vertical scalar flux for the RBSA (a,b,c), RBAA (d,e,f), and UBSA (g,h,i) configurations,.Solid lines represent the total scalar flux, broken lines represent the turbulent scalar flux and dotted lines represents the advective scalar flux. Capital letters indicates the urban zones (see Figures 1b,d,f).

Therefore, the turbulent and advective vertical fluxes are very important inside the canopy over the area source; however, as the distance from the source increases the turbulent vertical flux dominates and is stronger above the canopy. This means that the pollutants emitted in the area source are well transported vertically by advection inside the canopy over the area source but are more strongly influenced by the turbulent flux above the canopy further from the source. Compared to the staggered configurations, it can also be seen that the vertical fluxes remain important inside the canopy for longer distances from the source for the RBAA due to the channelling effect.

Spatially averaged horizontal total, advective and turbulent scalar fluxes are presented in Figure 11 for the three urban zones in all configurations. Horizontal scalar fluxes were spatially averaged at the outlet of the urban zones over a line at every $0.2H_m$ from the ground until $4H_m$ to produce a vertical profile. While advective fluxes are the dominant mechanism responsible for horizontal transport, vertical transport results from a complex interaction between turbulent and advective fluxes, especially for the configuration with random building heights. Over the area source (zone A), for the staggered configurations (Figures 11a and g) there is an increase of the horizontal scalar flux with height because there is less obstruction to the flow. It reaches its peak at the canopy top and after that, the horizontal scalar flux decreases with height. In contrast, for the aligned configuration (Figure 11d), there is a decrease of the horizontal scalar flux with height, since there is less channeling of the flow with height. Note that the turbulent horizontal scalar flux is negative for the three cases in the three urban zones.

Figure 12 presents the ratio between vertical and averaged horizontal fluxes leaving zone A. The horizontal fluxes were averaged for two different vertical planes: from the ground to $z/H_m = 1.0$ and also to $z/H_m = 1.72$. As discussed previously, the proportion between horizontal fluxes inside the canopy and the vertical flux to the atmosphere above is very important in setting the pollutant concentration in downwind areas, since it will indicate the ratio between the amounts of pollutant transported from the canopy to the atmosphere above and the amount of pollutant transported to the region downwind. In general, the staggered configurations (RBSA and UBSA) yield a larger ratio between vertical and horizontal fluxes for $z/H_m = 1.0$, which indicates that these configurations have stronger vertical mass transfers than the aligned configuration. This trend is probably related to the channeling effect caused by the aligned streets in the RBAA configuration.

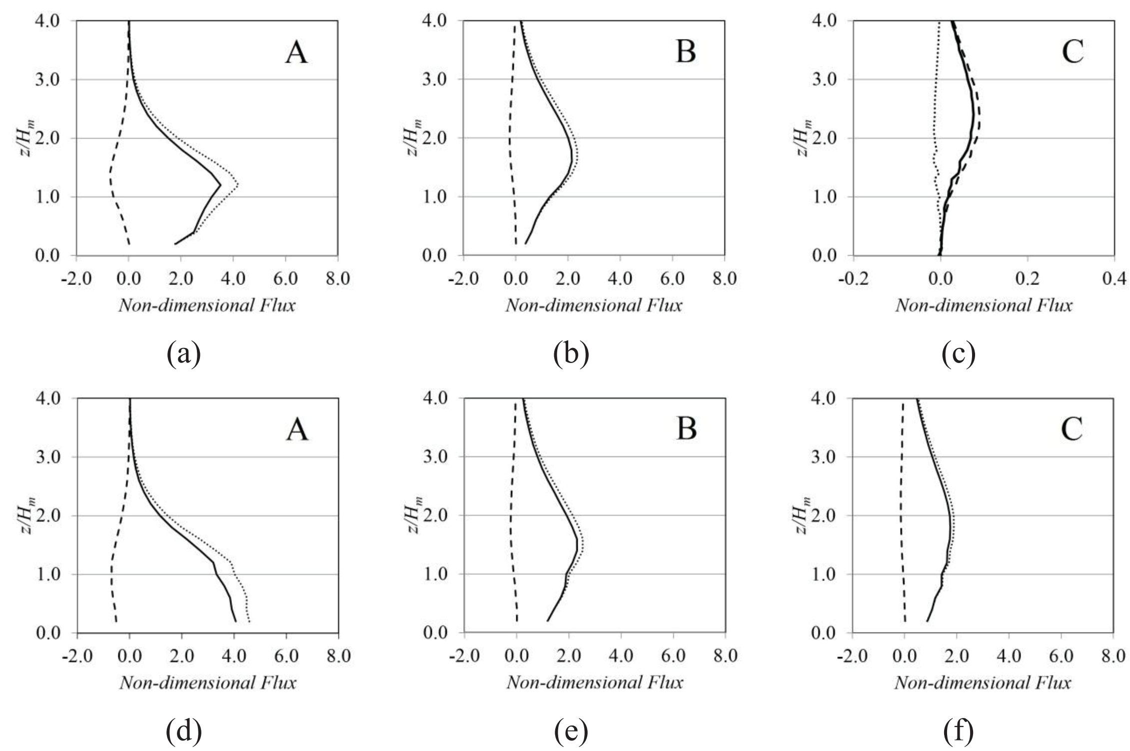

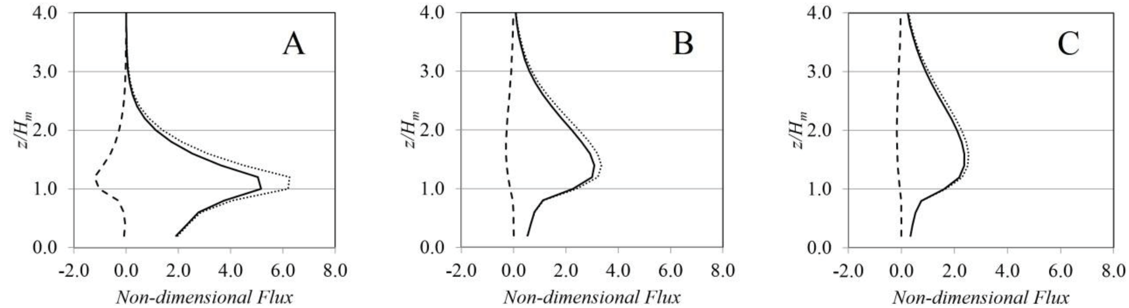

(g) (h) (i)

Figure 11. Spatially averaged vertical profile of horizontal scalar flux for RBSA (a,b,c) RBAA (d,e,f) and for UBSA (g,h,i) configurations. Solid lines represent the total scalar flux, broken lines represent the turbulent scalar flux and dotted lines represent the advective scalar flux. Capital letters indicates the urban zones (see Figure1b,d,f).

The configuration RBSA displays a ratio between vertical and horizontal fluxes larger than unity, which indicates that there is more mass leaving the canopy to the upper atmosphere than mass being transferred further downwind. The configuration UBSA also presents a ratio close to unity, but the value is more than 20% smaller than the value obtained for the RBSA configuration, which may indicate that random building heights play an important role in the process. For $z/H_m = 1.72$ a significant part of the scalar mass is still being transported upwards to the atmosphere in the cases with random building heights.

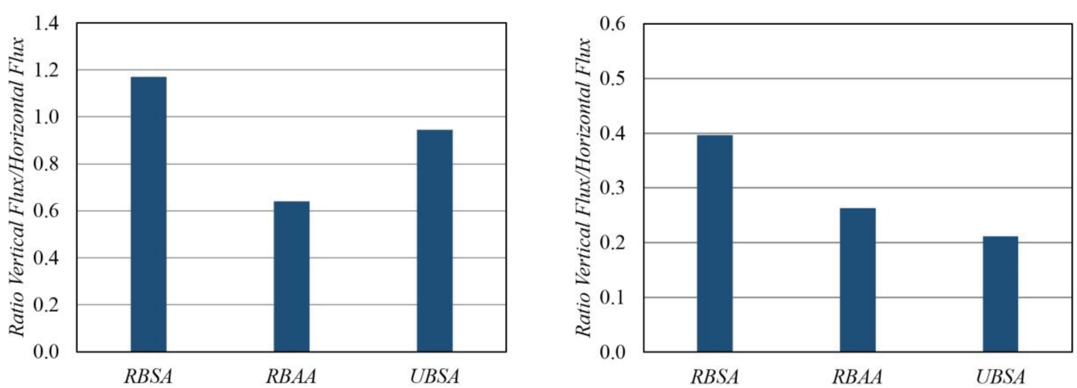

(a) (b)

Figure 12. Ratio between vertical and averaged horizontal fluxes leaving zone A, for (a) $z/H_m = 0$ to $z/H_m = 1.0$ and (b) $z/H_m = 0$ to $z/H_m = 1.72$.

4. Conclusions

The results demonstrate that the advective vertical scalar flux plays a very important role in the local transport of pollutants from/to the array, to an extent which varies according to building height differences and arrangements. In fact, in staggered array cases the advective vertical scalar flux has the same magnitude as the turbulent vertical scalar flux even in the case of uniform building heights. Moreover, the advective vertical scalar flux is negative in some locations, while the turbulent vertical scalar flux is always positive at all locations, enhancing and reducing, respectively, the concentration within the canopy.

In general, the staggered configurations (RBSA and UBSA) give a larger ratio between vertical and horizontal fluxes $at\ z/H_m = 1.0$, which indicates that these configurations yield stronger vertical mass transfer than the aligned configuration. This trend is probably related to the channeling effect caused by the aligned streets in the RBAA configuration.

For non-uniform heights arrays, there are intense down and up drafts in front of and behind the tall buildings. In addition, taller buildings promote an increase in the turbulent fluctuations of the vertical velocity above the smaller buildings. While the effects related to the mean flow are more local (close to the tall building), the effects related to the vertical velocity fluctuations, and consequentially the turbulent vertical fluxes, seem more largely spread downwind above the smaller buildings (a non-local effect).

It is important to highlight that although the local advective vertical scalar flux is important in the vicinity of the buildings, the spatially averaged vertical scalar flux indicates that the turbulent flux is dominant. Nonetheless, the local advective vertical scalar flux close to tall buildings remains important in determining the local concentration. This fact may prove to be a challenge for existing street network dispersion models that use the spatially average turbulent vertical scalar flux to parameterize the transfer velocity. Further research is needed on this topic.

Acknowledgements

This work was supported by the National Council for Scientific and Technological Development (CNPq) and Espírito Santo Research Foundation (FAPES) in Brazil and by the Newton Research Collaboration Programme Award NRCP1617-6-140, administered by the Royal Academy of Engineering as part of the UK Government's Newton Fund in UK. The first three authors acknowledge the hospitality provided by the Engineering Faculty of the University of Southampton during various extended visits as part of that Newton Fund support.

References

Aristodemou E, Boganegra LM, Mottet L, Pavlidis D, Constantinou A, Pain C, Robins A, ApSimon H. (2018) How tall buildings affect turbulent air flows and dispersion of pollution within a neighbourhood. Environmental Pollution, 233, 782-796

Boppana, V., Xie, Z.-T., and Castro, I. P. (2010). Large-eddy simulation of dispersion from surface sources in arrays of obstacles. Boundary layer meteorology, 135, 433-454.

Branford, S., Coceal, O., Thomas, T. G. and Belcher, S. E. (2011). Dispersion of a point-source release of a passive scalar through an urban-like array for different wind directions. Boundary Layer Meteorology, 363, 2947-2968.

Cai XM, Barlow JF, Belcher SE (2008) Dispersion and transfer of passive scalars in and above street canyons large-eddy simulations. Atmos Environ 42:5885–5895

Carpentieri, M., Robins, A. G. and Baldi, S. (2009). Three-dimensional mapping of air flow at an urban canyon intersection. Boundary Layer Meteorology, 133, 277-296.

Carpentieri, M., Robins, A. G., Hayden, P. and Santi, E. (2018). Mean and turbulent mass flux measurements in an idealised street network. Environmental Pollution, 234, 356-367.

Castro, I. P., Xie, Z.-T., V.Fuka, Robins, A. G., Carpentieri, M., Hayden, P., Hertwig, D. and Coceal, O. (2017). Measurements and computations of flow in an urban street system. Boundary Layer Meteorology, 162, 207-230.

Cheng, H. and Castro, I. P. (2002). Near wall ow over urban-like roughness. Boundary Layer Meteorology, 104, 229-259.

Coceal, O., Thomas, T. G., Castro, I. P. and Belcher, S. E. (2006). Mean flow and turbulent statistics over group of urban-like cubical obstacle. Boundary Layer Meteorology, 121, 491-519.

Coceal, O., Dobre, A., Thomas, T. G. and Belcher, S. E. (2007). Structure of turbulent flow over regular arrays of cubical roughness. Journal of Fluid Mechanics, 589, 375-409.

Coceal, O.; Goulart, E.V.; Branford, S.; Thomas, T.; Belcher, S.E, (2014). Flow structure and near-field dispersion in arrays of building-like obstacles. Journal of Wind Engineering and Industrial Aerodynamics, 125, 52-68

Davidson, M., Mylne, K.R., Jones, C.D., Phillips, J., Perkins, R.J., Jung, J. and Hunt, J. (1995). Plume dispersion through large groups of obstacles – a field investigation. Atmospheric Environment, 29, 3245-3256.

Fuka, V., Xie, Z.-T., Castro, I. P., Hayden, P., Carpentieri, M. and Robins, A. (2018). Scalar fluxes near a tall building in an aligned array of rectangular buildings. Boundary Layer Meteorology, 167, 103-124.

Goulart, E., Coceal, O., Branford, S., Thomas, T. G. and Belcher, S. (2016). Spatial and temporal variability of the concentration field from localized releases in a regular building array. Boundary-Layer Meteorology, 159, 241-257.

Goulart, E., Coceal, O. and Belcher, S. (2018). Dispersion of a passive scalar within and above an urban street network. Boundary-Layer Meteorology, 166, 241-257.

Hang J, Li YG. (2010) Ventilation strategy and air change rates in idealized high-rise compact urban areas. Building and Environment 45 (12): 2754-2767

Hang J, Li YG, Sandberg M. (2011) Experimental and numerical studies of flows through and within high-rise building arrays and their link to ventilation strategy. Journal of Wind Engineering and Industrial Aerodynamics, 99 (10): 1036-1055

J. Hang, Y. Li, M. Sandberg, R. Buccolieri, S. Di Sabatino, (2012) The influence of building height variability on pollutant dispersion and pedestrian ventilation in idealized high-rise urban areas, Building and Environment, 56, 346-360

Hertwig, D., Soulhac, L., Fuka, V.,Auerswald T., Carpentieri M., Hayden P., Robins A.G., Xie Z.T., Coceal O.. (2018) Evaluation of fast atmospheric dispersion models in a regular street network Environ. Fluid Mech..

Hilderman, T., Chong, R. and Kiel, D. (2004). Urban dispersion modelling data. Coanda Research and Development Corporation, 1, 1.

Kikumoto, H. and Ooka, R. (2018). Large-eddy simulation of pollutant dispersion in a cavity at fine grid resolutions. Building and Environment, 127, 127-137.

MacDonald, R., Grffiths, R.F. and Cheah, S.C. (1997). Field experiment of dispersion through regular array of cubic structure. Atmospheric Environment, 31, 783-795.

MacDonald, R., Griffiths, R. F. and Hall, D. J. (1998). A comparison of results from scaled field and wind tunnel modelling of dispersion in array of obstacles. Atmospheric Environment, 32, 3845-3862.

Pascheke, F., Barlow, J. and Robins, A. G. (2008). Wind-tunnel modelling of dispersion from a scalar area source in urban-like roughness. Boundary Layer Meteorology, 126, 103-124.

Phillips, D., Rossi, R. and Iaccarino, G. (2013). Large-eddy simulation of passive scalar dispersion in an urban-like canopy. Journal of Fluid Mechanics, 723, 404-428.

Smagorinsky, J. (1963) General circulation experiments with the primitive equations: I. The basic experiment. Monthly weather review, v. 91, n. 3, p. 99-164.

Tominaga, Y. and Stathopoulos, T. (2016). Ten questions concerning modelling of near-field pollutant dispersion in the built environment. Building and Environment, 105, 390-402.

Xie, Z.-T. and Castro, I. P. (2006). Les and rans for turbulent ow over arrays of wall-mounted obstacles. Flow Turbulence Combustion, 76, 291-312.

Xie, Z.-T., Coceal, O. and Castro, I. P. (2008). Large-eddy simulation of flows over random urban-like obstacles. Boundary Layer Meteorology, 129,1-23.

Xie ZT, Hayden P, Voke PR, Robins AG (2004) Large-eddy simulation of dispersion: comparison between elevated and ground-level sources. J*ournal of Turbulence* 5, 1–16

Yevgeny A. Gayev, Julian C.R. Hunt (2007). Flow and Transport Processes with Complex Obstructions: Applications to Cities, Vegetative Canopies and Industry. Springer Science & Business Media, Feb 6, 2007

Yoshida, T., Takemi, T., Horiguchi, M. (2018) Large-Eddy-Simulation Study of the Effects of Building-Height Variability on Turbulent Flows over an Actual Urban Area Boundary Layer Meteorology, 168, 127-153.

Yuan, C., Ng, E. and Norford, L. (2014). Improving air quality in high-density cities by understanding the relationship between air pollutant dispersion and urban morphologies. Building and Environment, 71, 245-258.

Zaki SA, Hagishima A, Tanimoto J, Ikegaya N (2011) Aerodynamic parameters of urban building arrays with random geometries. Boundary-Layer Meteorology 138(1), 99–120.